Neurovascular Unit Model

Documentation for Code Version 1.1

A merged NVC model of a neuron, astrocyte, smooth muscle cell, endothelial cell and the mechanical vessel response.

by Emiel van Disseldorp* , Katharina Dormanns† & Sanne van der Lelij‡

October 3, 2014

*University of Eindhoven, e.m.j.v.disseldorp@student.tue.nl
†University of Canterbury, katharina.dormanns@pg.canterbury.ac.nz
‡University of Eindhoven, s.m.v.d.lelij@student.tue.nl

Contents

1 Introduction

1.1 Neurovascular Unit

The cerebral cortex, a highly complex component of the human brain and part of the grey matter (*substantia grisea*), mainly consists of neurons (NEs), unmyelinated axons and glial cells such as astrocytes (ACs). It forms the outer layer of *cerebrum* and *cerebellum* and is veined with capillary blood vessels that provide the brain tissue with glucose and oxygen (Shipp [12]). These arterioles are surrounded by endothelial cells (ECs) that form a thin layer on the interior surface of arterioles (*intima*). The outer layer of the arteriole consists of smooth muscle cells (SMCs), which are aligned in circumferential direction. They define the contractile unit of the vessel and regulate its diameter by contraction and dilation.

A neurovascular unit (NVU) defined in this research includes one cell of each of the described types and is graphically pictured in Figure 1.

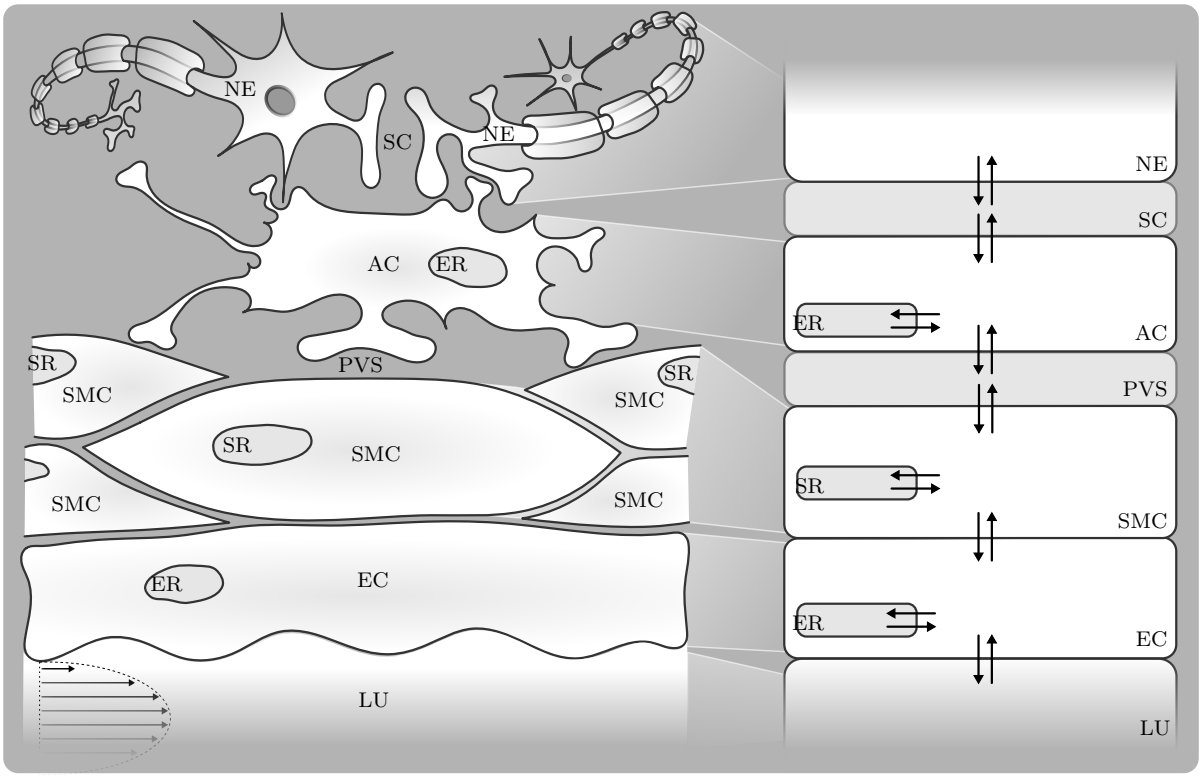

Figure 1: **Overview of different cells and domains that form a neurovascular unit.** NE - Neuron, SC - Synaptic Cleft, AC - Astrocyte, ER - Endoplasmic Reticulum, PVS - Perivascular Space, SMC - Smooth Muscle Cell, SR - Sarcoplasmic Reticulum, EC - Endothelial Cell, LU - Lumen with indicated blood flow. Intercellular communication via the exchange of ions is indicated by arrows.

Each of the cell types and the spaces in between play an important role within the process of neurovascular coupling (NVC, see Section 1.2). The synaptic cleft (SC) is the space between an axon terminal and dendrite of two different NEs in which neurotransmitters are released. It is enclosed by the star-shaped AC that can take up released neurotransmitters. Protoplasmic ACs are polarized cells which can temporarily buffer extracellular K^+, which is one of the key mechanisms within NVC. The astrocytic endoplasmatic reticulum (ER), an isolated space in the cytosol, contains IP_3-sensitive Ca^{2+} channels, which can release Ca^{2+}-ions into the cytosol. The perivascular space (PVS) is located between the end feet of an AC and the arteriole. In the PVS, ion exchange occurs between the arterial wall and the AC. The ECs form a monolayer on the luminal side of the vessel in which all cells are aligned in the direction of the flow. It prevents passive diffusion of bigger molecules, while small ones, such as O_2, Ca^{2+} or IP_3, can pass through. It also functions as an active organ sensing wall shear stress which plays an important role in the NO-mediated pathway. Together with the SMC layer the endothelium forms the blood brain barrier (BBB), the physical frontier between brain tissue and blood vessel. SMC contraction occurs by actin and myosin filaments forming cross-bridges. The rate of contraction is dependent on the SMC cytosolic Ca^{2+} concentration.

1.2 Neurovascular Coupling

Neurovascular coupling (NVC), or functional hyperaemia, describes the local vasodilation and -contraction due to neuronal activation. The change in the vessel diameter (vasoreactivity) controls the blood flow and thereby the cerebral supply of oxygen and glucose.

Each cell type plays an important specific role during the process of NVC. Communication between cells is based on an exchange of ions through pumps and channels. These ion fluxes contribute to changes in cytosolic and intercellular species concentration and cell membrane potentials.

There are several pathways that can lead to vasocontraction or -dilation and are mediated by different signalling molecules, such as K^+, Ca^{2+}, EET, NO and 20-HETE. Neurotransmitters are released by the NE into the SC and can bind to receptors on dendrites of other neurons and astrocytes. This leads to a cascade of chemical reactions and the opening and closing of ion channels which influences the fluxes and concentrations.

1.3 Mathematical Approach

The physiological models are based on a set of differential equations that describe the mass conservation of ions and molecules passing from one cell or domain to another. The simulations describe time-dependent ion fluxes and changes in membrane potential modelled by reaction rates that describe the kinetics which are physiologically validated by experimental data from the literature. This approach assumes homogeneous behaviour of a variable in a certain subdomain i.e. the spatial gradient of a variable in every subdomain is negligible.

2 Existing Models

The present mathematical model is the first of its kind, leading the way in modelling the whole neurovascular coupling process. Starting with the neuronal activation we build up to the response in vessel diameter, utilizing all cell types and crucial pathways. It is based on three existing models.

- **The Astrocyte Model** - describes the crucial biochemical processes within the astrocyte (AC, Østby et al. [11], reviewed by Donk and Kock [2]).
- **The SMC and EC Model** - describes the behaviour and the main ion fluxes within the smooth muscle cell (SMC) and endothelium cell (EC). This model is based on that of Koenigsberger et al. [10].
- **The Contraction and Mechanical Model** - describes the relationship between the cytosolic calcium (Ca^{2+}) concentration in the SMC and the contraction and dilation of the SMC by a myosin phosphorylation and cross-bridge based on the models of Hai and Murphy [8] and Kelvin Voigt.

2.1 The Astrocyte Model

During neural activity, K^+ is released into the synaptic cleft (SC) by active neurons (NEs). In the astrocyte model, this is implemented by an influx of K^+ (J_{K_s}) with a corresponding Na^+ uptake by the neuron (J_{Na_s}, Figure 2). The increase of K^+ in the SC results in an increased K^+ uptake by the AC which consequently undergoes depolarization. This results in a K^+ efflux from distant portions of the cell. Since most of the K^+ conductance of ACs is located at the end-feet, the outward current-carrying K^+ would flow out of the cell largely through these locations. Consequently, the K^+ is 'siphoned' to the end-feet of the astrocyte and released into the perivascular space (PVS) which leads to an increase of K^+ in the PVS. This K^+ release leads to a repolarization of the membrane voltage and is the input signal for the second (SMC & EC) part of this model.

The AC model contains different types of active and passive ion channels. These ion channels and pumps are captured in a set of differential equations to describe the conservation of mass for the corresponding species concentrations in the SC, the AC and the PVS. The ion channels for potassium (J_{KCC1}, J_{NKCC1}, J_K, J_{NaK} and J_{BK}), sodium (J_{NBC}, J_{NKCC1}, J_{NaK} and J_{Na}), chloride (J_{KCC1}, J_{NKCC1} and J_{Cl}) and bicarbonate (J_{HCO_3}) are included. Note that the bicarbonate and chlorine fluxes are coupled with the Na^+ and K^+ fluxes to obtain a neutral in- or efflux membrane voltage-wise.

The release of glutamate from the neuron in the synaptic cleft is simulated by creating a smooth pulse function ρ that describes the ratio of bound to total glutamate receptors on the synapse end of the astrocyte. This induces an IP_3 release into the cell, causing the release

of Calcium from the ER into the cytosol, which then leads to the production of EET. The K^+ release into the PVS is controled by the BK-channels. The opening of the BK-channels is regulated by the membrane voltage, as wel as the EET and Ca^{2+} concentration.

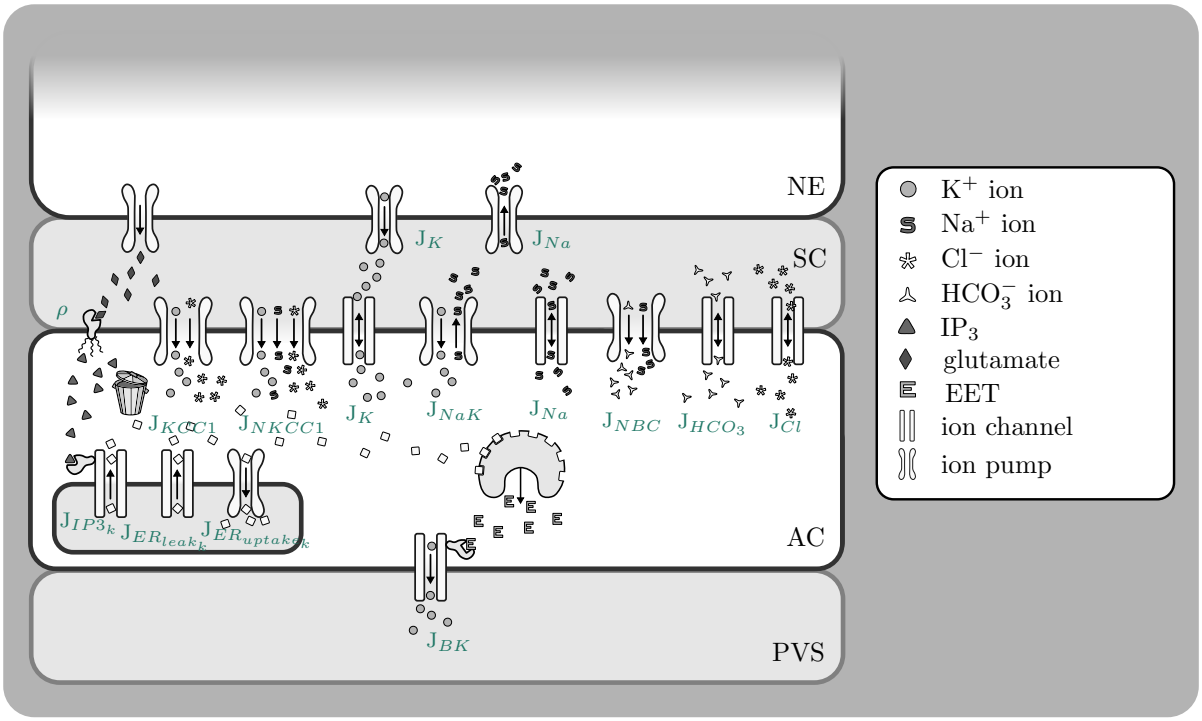

Figure 2: **Illustration of the astrocyte model.** All modelled fluxes are pictured, note that the indices (k - Astrocyte (AC), s - Synaptic Cleft (SC), p - Perivascular Space (PVS)) are left out for clarity reasons.

2.1.1 Input Signal

In this model, a neuronal excitation was mimicked by an efflux of K^+ into the synaptic cleft (SC) and a simultaneous equal influx of Na^+ into the neuron from the SC (Østby et al. [11], see equations in section 3.1.2). The time-dependent input signal ($f(t)$, see figure 3) starts at $t = 200s$ and ends at $t = 210s$. To estimate the profile $f(t)$ of the K^+ efflux/Na^+ influx, it is assumed that the K^+ efflux has a shape of a beta distribution with the governing parameters α and β such that the profile is optimized according to two criteria [11]:

1. The time from the start until the attaining maximum level of the K^+ concentration in the SC is 5s.

2. The level of the K^+ concentration in the SC at $t = 30$s is 60% of the minimal level.

These two criteria take into account that β is set at a value of $\beta = 5$.

In order to enhance the maximum K^+ level in the SC to reach the order of magnitude proposed by Filosa et al. [4], the amplitude of the input signal $f(t)$ is scaled up by the value F_{input}. The quantity of K^+ ions pumped into the AC can be derived by taking the integral of the flux $k_c f(t)$ over time, where k_c is a constant that relates the input signal $f(t)$ to the K^+ influx.

The amount of released ions are slowly buffered back by the neuron after the input signal terminates. This is modelled by a decay constant within the time interval $230s \leq t \leq 240s$. The integral of this block function is the same as the integral of the beta distribution in order to return to the baseline.

Beside this neuronal input signal, the NKCC1 and KCC1 co-transporters are only enabled when the neuronal ion release and spatial buffering are applied. With both parameters added, the behaviour is modelled by a block function with the value $-F_{input}$ with a default value of zero (Figure 3).

2.1.2 Scaling

The flux equations used in the AC model are based on the model of Østby et al. [11]. Their intention was to look at the volume changes of the AC and SC, therefore the volumes of both are variables in this model and all fluxes are scaled by a volume-surface ratio (R_k and R_s, see Equations 2 and 3, respectively). It is assumed that the sum of the volumes of the AC and SC is a constant (R_{tot}). Due to osmotic pressure, the volume changes. We could show that the changes are comparatively small in our model and it would be justifiable to leave out the scaling factors. However, at the moment they are included because the given fluxes of Østby et al. [11] are scaled by the volume-surface ratio. It should be considered in future versions to eliminate the scaling factors by multiplying the fluxes with an adequate constant.

2.2 SMC and EC Model

The SMC and EC model is based on the work of Koenigsberger et al. [10], see Figure 4. This model is extended by adding an inward-rectifier potassium (KIR) channel in the SMC (J_{KIR}, [4]) in order to create a connection between the Astrocyte model and the SMC and EC model.

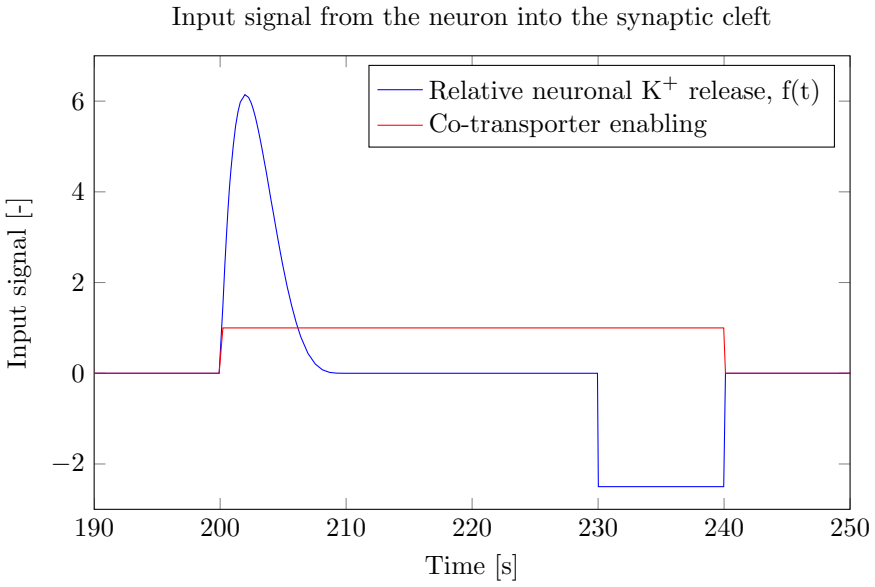

Figure 3: **The input signals used in the astrocyte model.** The K^+ efflux modelled by a beta distribution and buffered back afterwards (blue). The NKCC1 and KCC1 co-transporters are enabled when the neuronal ion release and spatial buffering is applied, modelled by a block function (red).

The input signal for this model is the K^+ concentration in the PVS which is increased by the efflux of astrocytic potassium after neuronal activity.

The raise in K^+ in the PVS activates the KIR channel on the SMC, causing them to open extruding more potassium into the PVS. This efflux of K^+ hyperpolarizes the SMC membrane and causing the voltage-operated Ca^{2+} channels to close, preventing the influx of Ca^{2+} into the SMC cytosol.

The cytosolic Ca^{2+} concentrations in the SMC and EC and that in the sacroplasmatic reticulum (SR) and endoplasmatic reticulum (ER), respectively, are described by a set of differential equations. In- and effluxes of K^+ are given by the following ion channel and pumps: J_{KIR}, J_{NaK} and J_K. Ca^{2+} leaves the SR via the channels: J_{CICR}, J_{IP_3} and J_{SR_leak} and enters it by J_{SR_upt}. The in- and efflux of Ca^{2+} are modelled with J_{extr}, J_{VOCC}, $J_{stretch}$ and J_{NaCa}. Note that these fluxes link the cytosol with the extracellular matrix. Here again, a chloride pump is included, J_{Cl}, to return to the resting membrane potential.

Physiologically, ECs and SMCs are connected by gap junctions that allow an intercellular exchange of molecules and voltage. Koenigsberger et al. [10] include the coupling factors $J^{EC-SMC}_{Ca^{2+}-cpl}$, V^{EC-SMC}_{cpl} and $J^{EC-SMC}_{IP_3-cpl}$ for Ca^{2+}, voltage and IP_3 coupling, respectively. The strength of the coupling can be changed in the code with the variable $CASE$.

Inositol triphosphate (IP_3) is an important messenger molecule. It's production, in the

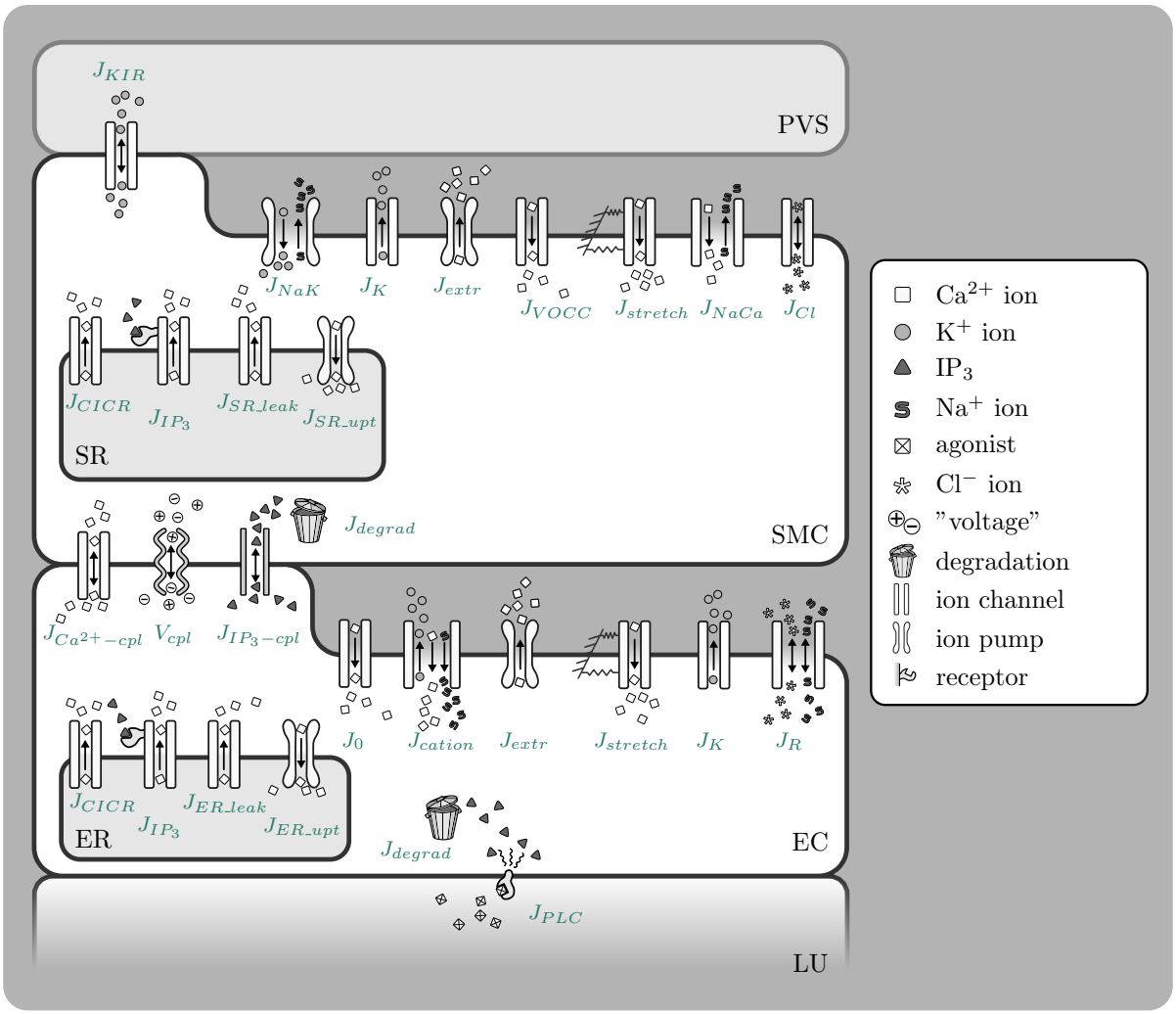

Figure 4: **Illustration of the SMC and EC model.** All modelled fluxes are pictured, note that the indices (k - Astrocyte (AC), s - Synaptic Cleft (SC), p - Perivascular Space (PVS)) are left out for clarity reasons.

endothelium, is triggered by agonist binding onto membrane receptors. IP_3 mediates the J_{IP_3} channel, situated between the reticulum and cytosol. The production rate of IP3 is a constant over time and can be changed by altering the variable J_{PLC} within the mathematical model .

Note that the model of Koenigsberger et al. [10] already includes Ca^{2+}-buffering in the SMC and EC.

2.3 Contraction and Mechanical Model

2.3.1 Contraction Model

The contraction and mechanical part of the model is based on the model of Hai and Murphy [8], which describes the formation of cross bridges between the myosin and actin filaments (Figure 5). This is coupled with a Kelvin-Voigt model that is used to describe the visco-elastic behaviour of the arterial wall (Figure 6).

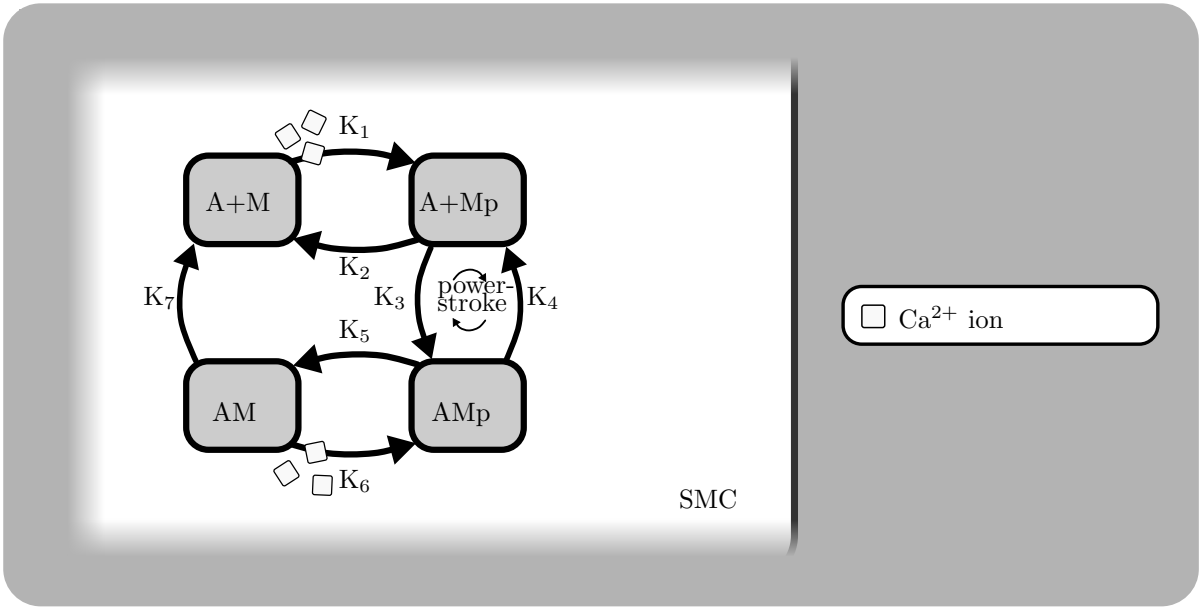

Figure 5: **Illustration of the contraction model within the smooth muscle cell.**

The Ca^{2+} concentration in the SMC is the input signal for the cross bridge model of Hai and Murphy [8]. The model uses four possible states for the formation of myosin: free nonphosphorylated cross bridges (M), free phosphorylated cross bridges (Mp), attached phosphorylated cross bridges (AMp) and attached dephosphorylated latch bridges (AM). The dynamics of the fraction of myosin in a particular state is given by four differential equations.

The active stress of the SMC is directly proportional to the fraction of attached cross bridges (AM and AMp). Using this model the relation between the cytosolic Ca^{2+} concentration and the active stress of the SMC can be derived.

2.3.2 Mechanical Model

The fraction of attached myosin cross bridges is the input signal for the visco-elastic mechanical model (Kelvin Voigt, Figure 6) which describes the changes in radius over time.

The pressure inside the vessel wall is taken as a constant and the circumferential stress is calculated using the Laplacian law.

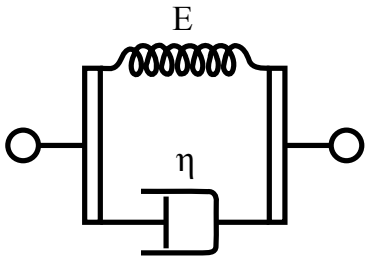

Figure 6: **Schematic overview of a Kelvin Voigt model.**

The Young's modulus and initial radius of the vessel wall is divided into an active and a passive part and is a function of the attached myosin cross-bridges. The active and passive Young's modulus are based and fitted on experimental data of Gore and Davis [7] which is shown in Figure 7.

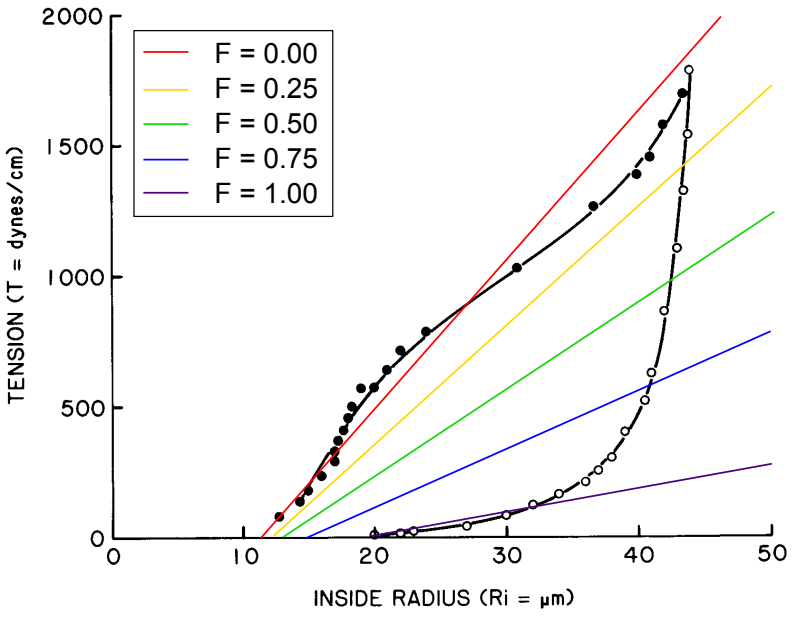

Figure 7: **Linearisation for the Young's modulus and initial radius on the data of Gore and Davis [7] for different values of F.**

Figure 7 shows that the initial radius (R_0) decreases when the fraction of attached myosin cross bridges (F) are increased (the intersection with the x-axis). The figure also shows that the Young's modulus, represented by the slope of the lines in the tension-strain graph,

increases when F increases. The linearisations of the Young's modulus can be described by:

$$T = \frac{\Delta T}{\Delta R}(R - R_0) \ , \tag{1}$$

where T is the tension of the vessel and $\frac{\Delta T}{\Delta R}$ is the slope of the linearisations in Figure 7.

2.4 Merging of All Models

The Astrocyte model and the SMC and EC model are linked by the SC and the PVS. The K^+ input signal of the neuron is pumped into the SC and taken up afterwards by the AC. The most important ion pumps and channels in this process are the K^+ channels in the neuron which releases the K^+ input, the Na^+/K^+ pump and K^+ channel in the AC which pump the released K^+ into the AC. The result of this is an efflux of K^+ at the end feet of the astrocyte using the BK-channel. Consequently, the membrane voltage of the astrocyte re-polarizes and the K^+ concentration in the PVS increases. This increased K^+ concentration activates the KIR channel in the SMC and start to pump out more K^+ from the SMC into the PVS. The increased efflux of K^+ hyperpolarises the SMC membrane voltage and as a result of that the VOCC closes and prevents the influx of Ca^{2+} into the SMC. Summarising, the neuronal input signal leads to a decrease of Ca^{2+} influx by the VOCC channels and therefore a decrease of the intracellular Ca^{2+} concentration. This leads to a decreased fraction of attached myosin bridges in the Hai and Murphy [8] model, resulting in vessel dilation in the visco-elastic mechanical model. An overview of the whole model is shown in Figure 8.

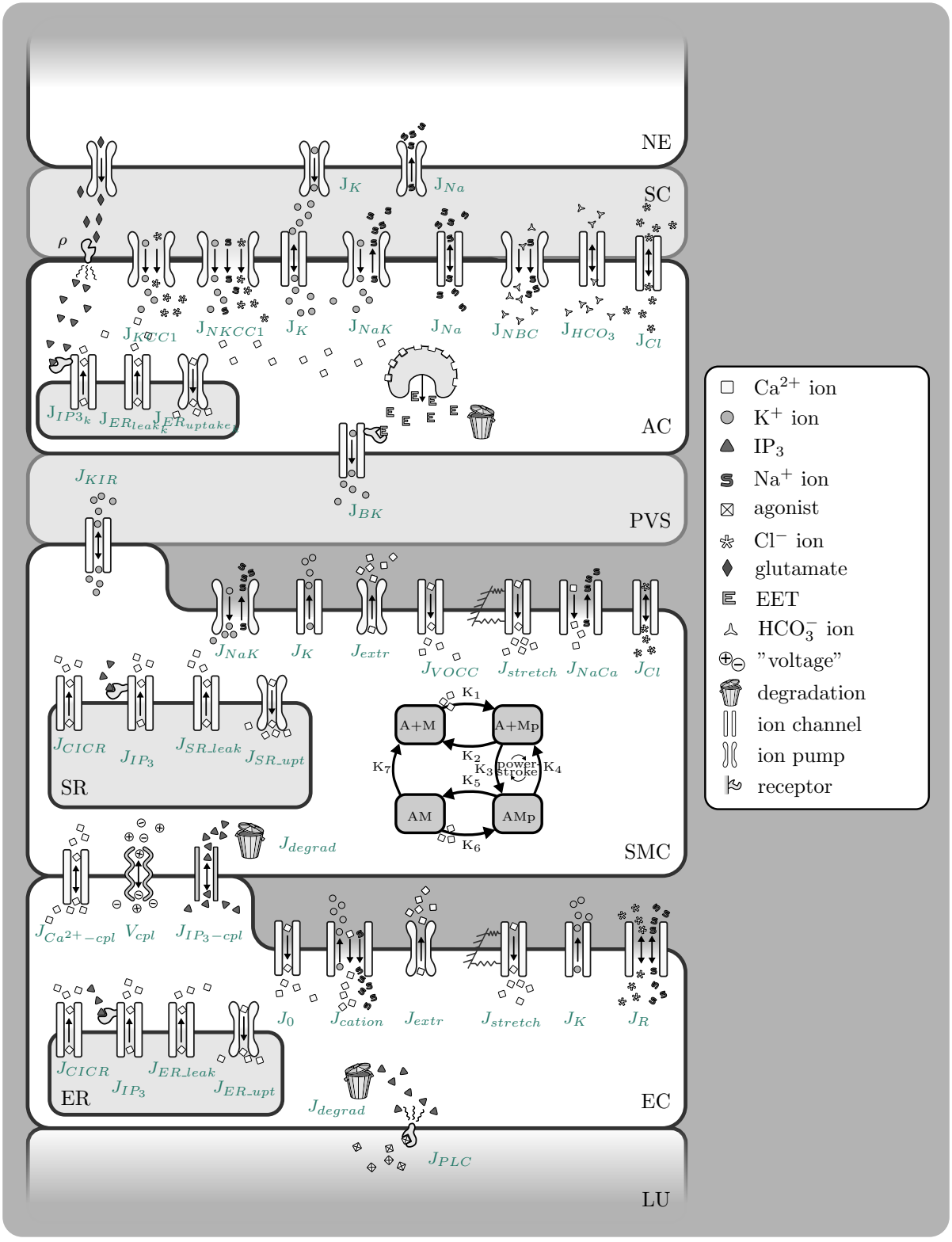

Figure 8: **All Models.**

3 Equations

3.1 Astrocyte Model

3.1.1 Scaling

The AC volume-area ratio (in m):

$$\frac{\mathrm{d}R_k}{\mathrm{d}t} = L_p \left(Na_k + K_k + Cl_k + HCO_{3_k} - Na_s - K_s - Cl_s - HCO_{3_s} + \frac{X_k}{R_k} \right) \tag{2}$$

The SC volume-surface ratio (in m):

$$R_s = R_{tot} - R_k \tag{3}$$

L_p	The total water permeability per unit area of the astrocyte	2.1e-9 mµM^{-1}s^{-1}	[11]
X_k	Number of negatively charged impermeable ions trapped within the astrocyte divided by the astrocyte membrane area	12.41e-3 µM m	[11]
R_{tot}	Total volume surface ratio AC+SC	8.79e-8 m	[11]

3.1.2 Input Signal

The neuronal K^+ input signal (-):
For $t < t_0$ and $t > t_3$:

$$f(t) = 0 \tag{4}$$

For $t_0 \leq t \leq t_1$:

$$f(t) = F_{input} \frac{(\alpha + \beta - 1)!}{(\alpha - 1)!(\beta - 1)!} \left(\frac{1 - (t - t_0)}{\Delta t} \right)^{\beta - 1} \left(\frac{t - t_0}{\Delta t} \right)^{\alpha - 1} \tag{5}$$

For $t_1 \leq t \leq t_2$:

$$f(t) = 0 \tag{6}$$

For $t_2 \leq t \leq t_3$:

$$f(t) = -F_{input} \tag{7}$$

ρ input signal The smooth pulse function ρ

$$\rho(t) = \frac{Amp - base}{2} \times \left(1 + \tanh \left(\frac{t - t_0}{\theta_L} \right) \right) + base + \frac{Amp - base}{2} \times \left(1 + \tanh \left(\frac{t - t_2}{\theta_R} \right) \right) + base - Amp \tag{8}$$

t_0	Start of neuronal pulse	200 s	ME
t_1	End of neuronal pulse	210 s	ME
t_2	Start of back-buffering	230 s	ME
t_3	End of back-buffering	240 s	ME
F_{input}	Amplitude scaling factor	2.5	ME
α	Beta-distribution constant	2	ME
β	Beta-distribution constant	5	ME
Δt	Time-scaling factor	10 s	ME
Amp	Amplitude of smooth pulse function	0.7	ME
$base$	Baseline of smooth pulse function	0.1	ME
θ_L	Left ramp of smooth pulse function	1	ME
θ_R	Left ramp of smooth pulse function	1	ME

3.1.3 Conservation Equations

Synaptic Cleft
K^+ concentration in the SC (times the SC volume-area ratio R_s; in µM m):

$$\frac{\mathrm{d}N_{K_s}}{\mathrm{d}t} = k_C f(t) - \frac{\mathrm{d}N_{K_k}}{\mathrm{d}t} - J_{BK_k} \tag{9}$$

Na^+ concentration in the SC (times the SC volume-area ratio R_s; in µM m):

$$\frac{\mathrm{d}N_{Na_s}}{\mathrm{d}t} = -k_C f(t) - \frac{\mathrm{d}N_{Na_k}}{\mathrm{d}t} \tag{10}$$

HCO_3 concentration in the SC (times the SC volume-area ratio R_s; in µM m):

$$\frac{\mathrm{d}N_{HCO_{3_s}}}{\mathrm{d}t} = -\frac{\mathrm{d}N_{HCO_{3_k}}}{\mathrm{d}t} \tag{11}$$

k_C	Input scaling parameter	7.35e-5 µM m s^{-1}	[11]

Astrocyte

K^+ concentration in the AC (times the AC volume-area ratio R_k; in µM m):

$$\frac{\mathrm{d}N_{K_k}}{\mathrm{d}t} = -J_{K_k} + 2J_{NaK_k} + J_{NKCC1_k} + J_{KCC1_k} - J_{BK_k} \tag{12}$$

Na^+ concentration in the AC (times the AC volume-area ratio R_k; in µM m):

$$\frac{\mathrm{d}N_{Na_k}}{\mathrm{d}t} = -J_{Na_k} - 3J_{NaK_k} + J_{NKCC1_k} + J_{NBC_k} \tag{13}$$

HCO_3 concentration in the AC (times the AC volume-area ratio R_k; in µM m):

$$\frac{\mathrm{d}N_{HCO_{3_k}}}{\mathrm{d}t} = 2J_{NBC_k} \tag{14}$$

Cl concentration in the AC (times the AC volume-area ratio R_k; in µM m):

$$\frac{\mathrm{d}N_{Cl_k}}{\mathrm{d}t} = \frac{\mathrm{d}N_{Na_k}}{\mathrm{d}t} + \frac{\mathrm{d}N_{K_k}}{\mathrm{d}t} - \frac{\mathrm{d}N_{HCO_{3_k}}}{\mathrm{d}t} \tag{15}$$

Ca^{2+} concentration in the astrocytic cytosol:

$$\frac{\mathrm{d}c_k}{\mathrm{d}t} = B_{\mathrm{cyt}}(J_{\mathrm{IP_3}} - J_{\mathrm{pump}} + J_{\mathrm{ER_leak}}) \tag{16}$$

Ca^{2+} concentration in the astrocytic ER:

$$\frac{\mathrm{d}s_k}{\mathrm{d}t} = \frac{1}{VR_{\mathrm{ER_{cyt}}}}(\frac{dc_k}{dt}) \tag{17}$$

The inactivation variable for IP_3:

$$\frac{\mathrm{d}h_k}{\mathrm{d}t} = k_{\mathrm{on}}[K_{\mathrm{inh}} - (c_k + K_{\mathrm{inh}})h_k] \tag{18}$$

The IP_3 concentration:

$$\frac{\mathrm{d}i_k}{\mathrm{d}t} = r_h G - k_{\mathrm{deg}} i_k \tag{19}$$

The EET concentration:

$$\frac{\mathrm{d}eetk_k}{\mathrm{d}t} = V_{\mathrm{eet}}(c_k - c_{\mathrm{k,min}}) - k_{\mathrm{eet}} eet_k \tag{20}$$

Open probability of the BK channel (s^{-1}):

$$\frac{\mathrm{d}w_k}{\mathrm{d}t} = \phi_w \left(w_\infty - w_k\right) \tag{21}$$

$VR_{\mathrm{ER_{cyt}}}$	Volume ratio of the ER to the cytosol in the astrocyte	0.185 [-]	[]
k_{on}	Rate of Ca^{2+} binding to the IP_3R	2 [µM s^{-1}]	[]
K_{inh}	Dissociation rate of k_{on}	0.1[µM]	[]
r_h	Maximum rate of IP_3 production in the astrocyte	4.8 [µM]	[]
k_{deg}	Rate constant for IP_3 degradation	1.25 [s^{-1}]	[]
V_{eet}	Rate constant for EET production	72 [µM]	[]
k_{eet}	Rate constant for EET degradation	7.2 [µM]	[]
$c_{\mathrm{k,min}}$	Minimum Ca^{2+} concentration required for EET production	0.1 [uM]	[]

Perivascular Space
K^+ concentration in the PVS (in µM):

$$\frac{\mathrm{d}K_p}{\mathrm{d}t} = \frac{J_{BK_k}}{R_k VR_{pa}} + \frac{J_{KIR_i}}{VR_{ps}} \tag{22}$$

VR_{pa}	Volume ratio of PVS to AC	0.001 [-]	[2]
VR_{ps}	Volume ratio of PVS to SMC	0.001 [-]	[2]

3.1.4 Fluxes

K^+ flux (times the AC volume-area ratio R_k; in µM m s^{-1}):

$$J_{K_k} = \frac{g_{K_k}}{F}(v_k - E_{K_k}) C_{correction} \tag{23}$$

Na^+ flux (times the AC volume-area ratio R_k; in µM m s^{-1}):

$$J_{Na_k} = \frac{g_{Na_k}}{F}(v_k - E_{Na_k}) C_{correction} \tag{24}$$

Na^+ and HCO_3 flux through the NBC channel (times the AC volume-area ratio R_k; in µM m s^{-1}):

$$J_{NBC_k} = \frac{g_{NBC_k}}{F}\left(v_k - E_{NBC_k}\right) C_{correction} \tag{25}$$

Cl and K^+ flux through the KCC1 channel (times the AC volume-area ratio R_k; in µM m s^{-1}):

$$J_{KCC1_k} = C_{input}\frac{g_{KCC1_k}}{F}\frac{RT}{F} ln\left(\frac{K_s Cl_s}{K_k Cl_k}\right) C_{correction} \tag{26}$$

Na^+, K^+ and Cl flux through the NKCC1 channel (times the AC volume-area ratio R_k; in µM m s^{-1}):

$$J_{NKCC1_k} = C_{input}\frac{g_{NKCC1_k}}{F}\frac{RT}{F} ln\left(\frac{Na_s K_s {Cl_s}^2}{Na_k K_k {Cl_k}^2}\right) C_{correction} \tag{27}$$

Flux through the sodium potassium pump (times the AC volume-area ratio R_k; in µM m s^{-1}):

$$J_{NaK_k} = J_{NaK_{max}}\frac{{Na_k}^{1.5}}{{Na_k}^{1.5} + {K_{Na_k}}^{1.5}}\frac{K_s}{K_s + K_{K_s}} \tag{28}$$

K^+ flux through the BK channel (times the AC volume-area ratio R_k; in µM m s^{-1}):

$$J_{BK_k} = \frac{g_{BK_k}}{F} w_k \left(v_k - E_{BK_k}\right) C_{correction} \tag{29}$$

Ca^{2+} flux from the ER to the cytosol in the astrocyte through IP_3 Receptors (IP_3R) by IP_3:

$$J_{\mathrm{IP3}} = J_{\max}[(\frac{i_k}{i_k + K_i})(\frac{c_k}{c_k + K_{\mathrm{act}}})h_k]^3 \times [1 - \frac{c_k}{s_k}] \tag{30}$$

The leakage Ca^{2+} flux from the ER to the cytosol in the astrocyte:

$$J_{\mathrm{ER_leak}} = P_L(1 - \frac{c_k}{s_k}) \tag{31}$$

The ATP dependent Ca^{2+} pump flux from the cytoplasm to the ER in the astrocyte:

$$J_{\mathrm{pump}} = V_{\max}\frac{c_k^2}{c_k^2 + k_p ump^2} \tag{32}$$

F	Faradays constant	9.649e4 C mol^{-1}	
R_g	Gas constant	8.315 J $mol^{-1}K^{-1}$	
T	Temperature	300 K	
g_{K_k}	Specific ion conductance of potassium	40 $\Omega^{-1}m^{-2}$	[11]
g_{Na_k}	Specific ion conductance of sodium	1.314 $\Omega^{-1}m^{-2}$	[11]
g_{NBC_k}	Specific ion conductance of the NBC cotransporter	7.57e-1 $\Omega^{-1}m^{-2}$	[11]
g_{KCC1_k}	Specific ion conductance of the KCC1 cotransporter	1e-2 $\Omega^{-1}m^{-2}$	[11]
g_{NKCC1_k}	Specific ion conductance of the NKCC1 cotransporter	5.54e-2 $\Omega^{-1}m^{-2}$	[11]
$J_{NaK_{max}}$	The maximum flux through the NaKATPase pump	1.42e-3 µMms^{-1}	[11]
g_{BK_k}	Specific ion conductance of the BK channel	1.16 $\Omega^{-1}m^{-2}$	[2]
$C_{correction}$	correction factor	10e3 [-]	[2]
C_{input}	Block function to switch the channel on and off	0 ; 1 [-]	[2]
J_{max}	Maximum IP_3 rate	2880 µM s^{-1}	[3]
K_I	Dissociation constant for IP_3 binding to IP_3R	0.03 µM	[3]
K_{act}	Dissociation constant for Ca^{2+} binding to IP_3R	0.17 µM	[3]
P_L	Associated with the steady state Ca^{2+} balance	5.2 µM	[3]
V_{max}	Maximal pumping rate of the Ca^{2+} pump	20 µM s^{-1}	[3]
k_{pump}	Dissociation constant of the Ca^{2+} pump	0.24 µM	[3]

3.1.5 Additional Equations

Synaptic Cleft
Cl concentration (times the SC volume-area ratio R_s; in µM m):

$$N_{Cl_s} = N_{Na_s} + N_{K_s} - N_{HCO_{3_s}} \tag{33}$$

Astrocyte
Membrane voltage of the AC (mV):

$$v_k = \frac{g_{Na_k}E_{Na_k} + g_{K_k}E_{K_k} + g_{Cl_k}E_{Cl_k} + g_{NBC_k}E_{NBC_k} + g_{BK_k}w_kE_{BK_k} - J_{NaK_k}FC_{correction}}{g_{Na_k} + g_{K_k} + g_{Cl_k} + g_{NBC_k} + g_{BK_k}w_k} \tag{34}$$

Nernst potential for the potassium channel (in mV):

$$E_{K_k} = \frac{R_gT}{z_KF}ln\left(\frac{K_s}{K_k}\right) \tag{35}$$

Nernst potential for the sodium channel (in mV):

$$E_{Na_k} = \frac{R_gT}{z_{Na}F}ln\left(\frac{Na_s}{Na_k}\right) \tag{36}$$

Nernst potential for the chloride channel (in mV):

$$E_{Cl_k} = \frac{R_gT}{z_{Cl}F}ln\left(\frac{Cl_s}{Cl_k}\right) \tag{37}$$

Nernst potential for the NBC channel (in mV):

$$E_{NBC_k} = \frac{R_g T}{z_{NBC} F} ln \left(\frac{Na_s {HCO_3}_s^2}{Na_k {HCO_3}_k^2} \right) \tag{38}$$

Nernst potential for the BK channel (in mV):

$$E_{BK_k} = \frac{R_g T}{z_K F} ln \left(\frac{K_p}{K_k} \right) \tag{39}$$

The Calcium buffering parameter in the astrocytic cytosol (-)

$$B_{cyt} = \left(1 + BK_{end} + \frac{K_{ex} B_{ex}}{(K_{ex} + c_k)^2} \right)^{-1} \tag{40}$$

The ratio of active to total G-protein (-)

$$G = \frac{\rho + \delta}{K_g + \rho + \delta} \tag{41}$$

Equilibrium state BK-channel (-):

$$w_\infty = 0.5 \left(1 + \tanh \left(\frac{v_k + (eet_{\text{shift}} eet_k) - v_3}{v_4} \right) \right) \tag{42}$$

The time constant associated with the opening of BK channels (in s^{-1}):

$$\phi_w = \psi_w \cosh \left(\frac{v_k - v_3}{2 v_4} \right) \tag{43}$$

Ca^{2+} dependent shift of the opening of the BK-channels

$$v_3 = \frac{v_5}{2} \tanh \left(\frac{c_k - Ca_3}{Ca_4} \right) + v_6 \tag{44}$$

g_{Cl_k}	Specific ion conductance of chloride	8.797e-1 $[\Omega^{-1}\mathrm{m}^{-2}]$	[11]
z_K	Valence of a potassium ion	1 [-]	
z_Na	Valence of a sodium ion	1 [-]	
z_Cl	Valence of a chloride ion	-1 [-]	
z_{NBC}	Effective valence of the NBC cotransporter complex	-1 [-]	
BK_{end}	Cytosolic endogenous buffer constant	40 [-]	[2]
K_{ex}	Cytosolic exogenous buffer dissociation constant	0.26 [µM]	[2]
B_{ex}	Concentration of cytosolic exogenous buffer	11.35 [µM]	[2]
δ	Ratio of the activities of the bound and unbound receptors	1.235e-3 [-]	[3]
K_G	The G-protein dissociation constant	8.82 [uM]	[3]
v_4	A measure of the spread of the distribution of the open probability of the BK channel	14.5e-3 [V]	[6]
v_5	Determines the range of the shift of n_{inf} as calcium varies	8e-3 [V]	[3]
v_6	The voltage associated with the opening of half the population	-15e-3 [V]	[3]
ψ_w	A characteristic time for the open probability of the BK channel	2.664 $[s^{-1}]$	[6]

3.2 SMC and EC Model

3.2.1 Conservation Equations

Smooth Muscle Cell

The cytosolic [Ca^{2+}] in the SMC (in µM):

$$\frac{\mathrm{d}[Ca^{2+}]_i}{\mathrm{d}t} = J_{IP_{3i}} - J_{SR_{uptake_i}} + J_{CICR_i} - J_{extrusion_i} + J_{SR_{leak_i}} \cdots - J_{VOCC_i} + J_{Na/Ca_i} + 0.1J_{stretch_i} + J^{SMC-EC}_{Ca^{2+}-coupling_i} \tag{45}$$

The [Ca^{2+}] in the SR of the SMC (in µM):

$$\frac{\mathrm{d}[\widehat{Ca}^{2+}]_i}{\mathrm{d}t} = J_{SR_{uptake_i}} - J_{CICR_i} - J_{SR_{leak_i}} \tag{46}$$

The membrane potential of the SMC (in mV):

$$\frac{\mathrm{d}v_i}{\mathrm{d}t} = \gamma_i(-J_{Na/K_i} - J_{Cl_i} - 2J_{VOCC_i} - J_{Na/Ca_i} - J_{K_i} \cdots - J_{stretch_i} - J_{KIR_i}) + V^{SMC-EC}_{coupling_i} \tag{47}$$

The open state probability of calcium-activated potassium channels (dimensionless):

$$\frac{\mathrm{d}w_i}{\mathrm{d}t} = \lambda_i \left(K_{act_i} - w_i\right) \tag{48}$$

The IP_3 concentration om the SMC (in µM):

$$\frac{\mathrm{d}[IP_3]_i}{\mathrm{d}t} = J^{SMC-EC}_{IP_3-coupling_i} - J_{degrad_i} \tag{49}$$

The K^+ concentration in the SMC (in µM):

$$\frac{\mathrm{d}[K_i^+]}{\mathrm{d}t} = J_{Na/K_i} - J_{KIR_i} - J_{K_i} \tag{50}$$

γ_i	The change in membrane potential by a scaling factor	1970 mVµM^{-1}	[10]
λ_i	The rate constant for opening	45.0 s^{-1}	[10]

Endothelial Cell
The cytosolic Ca^{2+} concentration in the EC (in µM):

$$\begin{aligned}\frac{\mathrm{d}[Ca^{2+}]_j}{\mathrm{d}t} = J_{IP_{3j}} - J_{ER_{uptake_j}} + J_{CICR_j} - J_{extrusion_j} \dots \\ + J_{ER_{leak_j}} + J_{cation_j} + J_{0_j} + J_{stretch_j} - J^{SMC-EC}_{Ca^{2+}-coupling_j}\end{aligned} \tag{51}$$

The Ca^{2+} concentration in the ER in the EC (in µM):

$$\frac{\mathrm{d}[\widehat{Ca}^{2+}]_j}{\mathrm{d}t} = J_{SR_{uptake_j}} - J_{CICR_j} - J_{SR_{leak_j}} \tag{52}$$

The membrane potential of the EC (in mV):

$$\frac{\mathrm{d}v_j}{\mathrm{d}t} = -\frac{1}{C_{m_j}}(J_{K_j} + J_{R_j}) + V^{SMC-EC}_{coupling_j} \tag{53}$$

The IP_3 concentration of the EC (in µM):

$$\frac{\mathrm{d}[IP_3]_j}{\mathrm{d}t} = J_{agonist_j} - J_{degrad_j} - J^{SMC-EC}_{IP_3-coupling_j} \tag{54}$$

C_{m_j}	Membrane capacitance	25.8 pF	[10]

3.2.2 Fluxes

Smooth Muscle Cell
The release of calcium from IP_3 sensitive stores in the SMC (in µM s^{-1}):

$$J_{IP_{3i}} = F_i \frac{[IP_3]_i^2}{K_{ri}^2 + [IP_3]_i^2} \tag{55}$$

F_i	Maximal rate of activation-dependent calcium influx	0.23 µM s^{-1}	[10]
K_{ri}	Half-saturation constant for agonist-dependent calcium entry	1 µM	[10]

The uptake of calcium into the sarcoplasmic reticulum (in µM s^{-1}):

$$J_{SR_{uptake_i}} = B_i \frac{[Ca^{2+}]_i^2}{c_{bi}^2 + [Ca^{2+}]_i^2} \tag{56}$$

B_i	SR uptake rate constant	2.025 µM s^{-1}	[10]
c_{bi}	Half-point of the SR ATPase activation sigmoidal (oder Michaelis (Menten) constant)	1.0 µM	[10]

The calcium-induced calcium release (CICR; in µM s^{-1}):

$$J_{CICR_i} = C_i \frac{[\widehat{Ca}^{2+}]_i^2}{s_{ci}^2 + [\widehat{Ca}^{2+}]_i^2} \frac{[Ca^{2+}]_i^4}{c_{ci}^4 + [Ca^{2+}]_i^4} \tag{57}$$

C_i	CICR rate constant	55 µM s^{-1}	[10]
s_{ci}	Half-point of the CICR Ca^{2+} efflux sigmoidal	2.0 µM	[10]
c_{ci}	Half-point of the CICR activation sigmoidal	0.9 µM	[10]

The calcium extrusion by Ca^{2+}-ATPase pumps (in µM s^{-1}):

$$J_{extrusion_i} = D_i[Ca^{2+}]_i \left(1 + \frac{v_i - v_d}{R_{di}}\right) \tag{58}$$

D_i	Rate constant for Ca^{2+} extrusion by the ATPase pump	0.24 s^{-1}	[9]
v_d	Intercept of voltage dependence of extrusion ATPase	-100.0 mV	[10]
R_{di}	Slope of voltage dependence of extrusion ATPase.	250.0 mV	[10]

The leak current from the SR (in µM s^{-1}):

$$J_{SR_{leak_i}} = L_i[\widehat{Ca}^{2+}]_i \tag{59}$$

L_i	Leak from SR rate constant	0.025 s^{-1}	[10]

The calcium influx through VOCCs (in µM s^{-1}):

$$J_{VOCC_i} = G_{Cai} \frac{v_i - v_{Ca_{1i}}}{1 + exp(-\left[\left(v_i - v_{Ca_{2i}}\right)/R_{Cai}\right])} \tag{60}$$

G_{Cai}	Whole-cell conductance for VOCCs	1.29e-3 µM $mV^{-1}s^{-1}$	[10]
$v_{Ca_{1i}}$	Reversal potential for VOCCs	100.0 mV	[10]
$v_{Ca_{2i}}$	Half-point of the VOCC activation sigmoidal	-24.0 mV	ME
R_{Cai}	Maximum slope of the VOCC activation sigmoidal	8.5 mV	[10]

The flux of calcium exchanging with sodium in the Na^+Ca^{2+} exchange (in µM s^{-1}):

$$J_{Na/Ca_i} = G_{Na/Ca_i} \frac{[Ca^{2+}]_i}{[Ca^{2+}]_i + c_{Na/Cai}} \left(v_i - v_{Na/Ca_i}\right) \tag{61}$$

$G_{Na/Cai}$	Whole-cell conductance for Na^+/Ca^{2+} exchange	3.16e-3 µM $mV^{-1}s^{-1}$	[9]
$c_{Na/Cai}$	Half-point for activation of Na^+/Ca^{2+} exchange by Ca^{2+}	0.5 µM	[10]
$v_{Na/Cai}$	Reversal potential for the Na^+/Ca^{2+} exchanger	-30.0 mV	[10]

The calcium flux through the stretch-activated channels in the SMC (in µM s^{-1}):

$$J_{stretch_i} = \frac{G_{stretch}}{1 + exp\left(-\alpha_{stretch}\left(\frac{\Delta pR}{h} - \sigma_0\right)\right)} \left(v_i - E_{SAC}\right) \tag{62}$$

$G_{stretch}$	The whole cell conductance for SACs	6.1e-3 µM $mV^{-1}s^{-1}$	[10]
$\alpha_{stretch}$	Slope of stress dependence of the SAC activation sigmoidal	7.4e-3 $mmHg^{-1}$	[10]
Δp	Pressure difference	30 mmHg	ME
σ_0	Half-point of the SAC activation sigmoidal	500 mmHg	[10]
E_{SAC}	The reversal potential for SACs	-18 mV	[10]

Flux through the sodium potassium pump (in µM s^{-1}):

$$J_{NaK_i} = F_{NaK} \tag{63}$$

F_{NaK}	Rate of the potassium influx by the sodium potassium pump	4.32e-2 µM s^{-1}	[10]

Chloride flux through the chloride channel (in µM s^{-1}):

$$J_{Cl_i} = G_{Cli}\,(v_i - v_{Cli}) \tag{64}$$

G_{Cli}	Whole-cell conductance for Cl^- current	1.34e-3 µM $mV^{-1}s^{-1}$	[10]
v_{Cli}	Reversal potential for Cl^- channels.	-25.0 mV	[10]

Potassium flux through potassium channel (in µM s^{-1}):

$$J_{K_i} = G_{Ki} w_i\,(v_i - vK_i) \tag{65}$$

G_{Ki}	Whole-cell conductance for K^+ efflux.	4.46e-3 µM $mV^{-1}s^{-1}$	[9]
vK_i	Nernst potential	-94 mV	[9]

The flux through KIR channels in the SMC (in µM s^{-1}):

$$J_{KIR_i} = \frac{F_{KIR_i} g_{KIR_i}}{\gamma_i}(v_i - v_{KIR_i}) \tag{66}$$

F_{KIR_i}	Scaling factor of potassium efflux through the KIR channel	7.5e2	[2]

The IP_3 degradation (in µM s^{-1}):

$$J_{degrad_i} = k_{di} I_i \tag{67}$$

k_{di}	Rate constant of IP_3 degradation	0.1 s^{-1}	[10]

Endothelial Cell

The release of calcium from IP_3-sensitive stores in the EC (in µM s^{-1}):

$$J_{IP_{3j}} = F_j \frac{[IP_3]_j^2}{K_{rj}^2 + [IP_3]_j^2} \tag{68}$$

F_j	Maximal rate of activation-dependent calcium influx	0.23 µM s^{-1}	[10]
K_{rj}	Half-saturation constant for agonist-dependent calcium entry	1 µM	[10]

The uptake of calcium into the endoplasmic reticulum (in µM s^{-1}):

$$J_{ER_{uptake_j}} = B_j \frac{[Ca^{2+}]_j^2}{c_{bj}^2 + [Ca^{2+}]_j^2} \tag{69}$$

B_j	ER uptake rate constant	0.5 µM s^{-1}	[10]
c_{bj}	Half-point of the SR ATPase activation sigmoidal (oder Michaelis (Menten) constant)	1.0 µM	[10]

The calcium-induced calcium release (CICR; in µM s^{-1}):

$$J_{CICR_j} = C_j \frac{[\widehat{Ca}^{2+}]_j^2}{s_{cj}^2 + [\widehat{Ca}^{2+}]_j^2} \frac{[Ca^{2+}]_j^4}{c_{cj}^4 + [Ca^{2+}]_j^4} \tag{70}$$

C_j	CICR rate constant	5 µM s^{-1}	[10]
s_{cj}	Half-point of the CICR Ca^{2+} efflux sigmoidal	2.0 µM	[10]
c_{cj}	Half-point of the CICR activation sigmoidal	0.9 µM	[10]

The calcium extrusion by Ca^{2+}-ATPase pumps (in µM s^{-1}):

$$J_{extrusion_j} = D_j [Ca^{2+}]_j \tag{71}$$

D_j	Rate constant for Ca^{2+} extrusion by the ATPase pump	0.24 s^{-1}	[9]

The calcium flux through the stretch-activated channels in the EC (in µM s^{-1}):

$$J_{stretch_j} = \frac{G_{stretch}}{1 + e^{-\alpha_{stretch}(\sigma - \sigma_0)}} (v_j - E_{SAC}) = \frac{G_{stretch}}{1 + e^{-\alpha_{stretch}\left(\frac{\Delta pR}{h} - \sigma_0\right)}} (v_j - E_{SAC}) \tag{72}$$

$G_{stretch}$	The whole cell conductance for SACs	6.1e-3 µM $mV^{-1}s^{-1}$	[10]
$\alpha_{stretch}$	Slope of stress dependence of the SAC activation sigmoidal	7.4e-3 $mmHg^{-1}$	[10]
Δp	Pressure difference	30 mmHg	ME
σ_0	Half-point of the SAC activation sigmoidal	500 mmHg	[10]
E_{SAC}	The reversal potential for SACs	-18 mV	[10]

The leak current from the ER (in µM s^{-1}):

$$J_{ER_{leak_j}} = L_j[\widehat{Ca}^{2+}]_j \tag{73}$$

L_j	Rate constant for Ca^{2+} leak from the ER	0.025 s^{-1}	[10]

The calcium influx through nonselective cation channels (in µM s^{-1}):

$$J_{cation_j} = G_{cat_j}(E_{Ca_j} - v_j)\frac{1}{2}\left(1 + \tanh\left(\frac{\log_{10}[Ca^{2+}]_j - m_{3_{cat_j}}}{m_{4_{cat_j}}}\right)\right) \tag{74}$$

G_{catj}	Whole-cell cation channel conductivity	6.6e-4 µM $mV^{-1}s^{-1}$	[10]
E_{Caj}	Ca^{2+} equilibrium potential	50 mV	[10]
$m_{3_{catj}}$	Model constant	-6.18 µM	[10]
$m_{4_{catj}}$	Model constant	0.37 µM	[10]

The potassium efflux through the $J_{BK_{Caj}}$ channel and the $J_{SK_{Caj}}$ channel (in µM s^{-1}):

$$J_{K_j} = G_{totj}(v_j - v_{Kj})\left(J_{BK_{Caj}} + J_{SK_{Caj}}\right) \tag{75}$$

G_{totj}	Total potassium channel conductivity.	6927 pS	[10]
v_{Kj}	K^+ equilibrium potential	-80.0 mV	[10]

The potassium efflux through the $J_{BK_{Caj}}$ channel (in µM s^{-1}):

$$J_{BK_{Caj}} = 0.2\left(1 + \tanh\left(\frac{(\log_{10}[Ca^{2+}]_j - c)(v_j - b_j) - a_{1j}}{m_{3bj}(v_j + a_{2j}(\log_{10}[Ca^{2+}]_j - c) - b_j)^2 + m_{4bj}}\right)\right) \tag{76}$$

The potassium efflux through the $J_{SK_{Caj}}$ channel (in µM s^{-1}):

$$J_{SK_{Caj}} = 0.3\left(1 + \tanh\left(\frac{\log_{10}[Ca^{2+}]_j - m_{3sj}}{m_{4sj}}\right)\right) \tag{77}$$

c	Model constant, further explanation see reference	-6.4 µM	[10]
b_j	Model constant, further explanation see reference	-80.8 mV	[10]
a_{1j}	Model constant, further explanation see reference	53.3 µM mV	[10]
a_{2j}	Model constant, further explanation see reference	53.3 mVµM^{-1}	[10]
m_{3bj}	Model constant, further explanation see reference	1.32e-3 µM mV^{-1}	[10]
m_{4bj}	Model constant, further explanation see reference	0.30 µM mV	[10]
m_{3sj}	Model constant, further explanation see reference	-0.28 µM	[10]
m_{4sj}	Model constant, further explanation see reference	0.389 µM	[10]

The residual current regrouping chloride and sodium current flux (in µM s^{-1}):

$$J_{R_j} = G_{R_j}(v_j - v_{restj}) \tag{78}$$

G_{R_j}	Residual current conductivity	955 pS	[10]
v_{restj}	Membrane resting potential	-31.1 mV	[10]

The IP_3 degradation (in µM s^{-1}):

$$J_{degrad_j} = k_{dj}[IP_3]_j \tag{79}$$

k_{dj}	Rate constant of IP_3 degradation	0.1 s^{-1}	[10]

3.2.3 Coupling

The heterocellular electrical coupling between SMCs en ECs (in mV s^{-1}):

$$V_{coupling_i}^{SMC-EC} = -G_{coup}(v_i - v_j) \tag{80}$$

The heterocellular IP_3 coupling between SMCs and ECs (in µM s^{-1}):

$$J_{IP_3-coupling_i}^{SMC-EC} = -P_{IP_3}([IP_3]_i - [IP_3]_j) \tag{81}$$

Calcium coupling with EC (inµM s^{-1}):

$$J_{Ca^{2+}-coupling_i}^{SMC-EC} = -P_{Ca^{2+}}([Ca^{2+}]_i - [Ca^{2+}]_j) \tag{82}$$

$P_{CA^{2+}}$	Heterocellular $P_{Ca^{2+}}$ coupling coefficient	0.05 s^{-1}	[10]
P_{IP_3}	Heterocellular IP_3 coupling coefficient	0.05 s^{-1}	[10]
G_{coup}	Heterocellular electrical coupling coefficient	5 s^{-1}	ME

3.2.4 Additional Equations

The equilibrium distribution of open channel states for the voltage and calcium activated potassium channels (dimensionless):

$$K_{act_i} = \frac{\left([Ca^{2+}]_i + c_{wi}\right)^2}{\left([Ca^{2+}]_i + c_{wi}\right)^2 + \beta_i exp(-\left([v_i - v_{Ca_{3i}}]\,/R_{Ki}\right))} \tag{83}$$

Nernst potential of the KIR channel in the SMC (in mV):

$$v_{KIR_i} = z_1 K_p - z_2 \tag{84}$$

Conductance of KIR channel (in s^{-1}):

$$g_{KIR_i} = exp(z_5 v_i + z_3 K_p - z_4) \tag{85}$$

c_{wi}	Translation factor for Ca^{2+} dependence of K_{Ca} channel activation sigmoidal.	0.0 µM	[10]
β_i	Translation factor for membrane potential dependence of K_{Ca} channel activation sigmoidal.	0.13 μM^2	[10]
$v_{Ca_{3i}}$	Half-point for the K_{Ca} channel activation sigmoidal.	-27 mV	[10]
R_{Ki}	Maximum slope of the K_{Ca} activation sigmoidal.	12 mV	[10]
z_1	Model estimation for membrane voltage KIR channel	4.5e3 mV	[2]
z_2	Model estimation for membrane voltage KIR channel	112 mV	[2]
z_3	Model estimation for the KIR channel conductance	4.2e2 µM $mV^{-1}s^{-1}$	[2]
z_4	Model estimation for the KIR channel conductance	12.6 µM $mV^{-1}s^{-1}$	[2]
z_5	Model estimation for the KIR channel conductance	-7.4e-2 µM $mV^{-1}s^{-1}$	[2]

3.3 Contraction and Mechanical Model

3.3.1 Contraction Equations

The fraction of free phosphorylated cross-bridges (dimensionless):

$$\frac{\mathrm{d}[Mp]}{\mathrm{d}t} = K_4[AMp] + K_1[M] - (K_2 + K_3)[Mp] \tag{86}$$

The fraction of attached phosphorylated cross-bridges (dimensionless):

$$\frac{\mathrm{d}[AMp]}{\mathrm{d}t} = K_3[Mp] + K_6[AM] - (K_4 + K_5)[AMp] \tag{87}$$

The fraction of attached dephosphorylated cross-bridges (dimensionless):

$$\frac{\mathrm{d}[AM]}{\mathrm{d}t} = K_5[AMp] - (K_7 + K_6)[AM] \tag{88}$$

The fraction of free non-phosphorylated cross-bridges (dimensionless):

$$[M] = 1 - [AM] - [AMp] - [Mp] \tag{89}$$

The rate constants that represent phosphorylation of M to Mp and of AM to AMp by the active myosin light chain kinase (MLCK), respectively (in s^{-1}):

$$K_1 = K_6 = \gamma_{cross}[Ca^{2+}]_i^3 \tag{90}$$

K_2	The rate constant for dephosphorylation (of Mp to M) by myosin light-chain phosphatase (MLCP)	0.5 s^{-1}	[8]
K_3	The rate constants representing the attachment/detachment of fast cycling phosphorylated crossbridges	0.4 s^{-1}	[8]
K_4	The rate constants representing the attachment/detachment of fast cycling phosphorylated crossbridges	0.1 s^{-1}	[8]
K_5	The rate constant for dephosphorylation (of AMp to AM) by myosin light-chain phosphatase (MLCP)	0.5 s^{-1}	[8]
K_7	The rate constant for latch-bridge detachment	0.1 s^{-1}	[8]
γ_{cross}	The sensitivity of the contractile apparatus to calcium	17 μM^{-3} s^{-1}	[8]

3.3.2 Mechanical Equations

The wall thickness of the vessel (in µm):

$$h = -0.1R \tag{91}$$

The fraction of attached myosin cross-bridges (dimensionless):

$$F_r = [AM_p] + [AM] \tag{92}$$

The vessel radius (in µm):

$$\frac{\mathrm{d}R}{\mathrm{d}t} = \frac{R_{0_{pas}}}{\eta}\left(\frac{RP_T}{h} - E(F_r)\frac{R - R_0(F_r)}{R_0(F_r)}\right) \tag{93}$$

with:

$$E(F_r) = E_{pas} + F_r\left(E_{act} - E_{pas}\right) \tag{94}$$

$$R_0(F_r) = R_{0_{pas}} + F_r(\alpha - 1)R_{0_{pas}} \tag{95}$$

η	viscosity	1e4 Pa s	[10]
$R_{0_{pas}}$	Radius of the vessel when passive and no stress is applied	20 µm	ME
$h_{0_{pas}}$	Wall thickness when passive and no stress is applied	3 µm	ME
P_T	Transmural pressure	4000 Pa	ME
E_{pas}	Young's moduli for the passive vessel	66e3 Pa	[7]
E_{act}	Young's moduli for the active vessel	233e3 Pa	[7]
α	Scaling factor initial radius	0.6	[7]

4 Code Structure

The main script of the code is named *'NVC_main.m'* and calls all the needed functions and other scripts. A graphic structure diagram is given in Figure 9.
'all_constants.m' contains all variables used in the model and is created to give a clear overview and furthermore to make it easy to recognize if variables are defined twice in the code inadvertently. In *'all_indices.m'* indices are defined for all differential equations (stored in the structure *ind*) and all fluxes (stored in the structure *flu*).

The fluxes and other non-differential equations are stored in *'all_fluxes.m'*. Here, a separate array is defined for each cell (NE, AC, SMC, EC) to create a clearly arranged structure. The indices refer to the corresponding cell type or domain (NE - n, AC - k, SMC - i, EC - j).
The mass conservation equations describing the time-dependent rate of change for each species concentration and membrane voltage, respectively, are stored in *'DEsyst.m'*. In the main script an ODE solver with adjustable options is chosen to solve the set of ordinary differential equations. The solution for each iteration step and the corresponding time are stored in the two variables *state* and *time*, respectively. The functions *'odeprog()'* and *'odeabort()'* [5] give a GUI with a visual progress bar to show the approximate remaining time and allow to abort the equation solving process via the *'Abort'*-button. After each iteration step the function *'writeFlux()'* is called to write each flux and ode solution, the corresponding flowrate (right hand side of the ODE) and time step into the array structure $DATA$. The stored values are used by the function *'plot_all.m'* to plot different state variables or fluxes.
The values of the two global variables $CASE$ and J_PLC can be changed in the main script in order to obtain different coupling strengths and binding agonist concentration, respectively. Also the value of NVU can be varied to execute either the NVU 1.0 of the NVU 1.1 model or look at the separate effects of Calcium and EET on the BK-channel open state.

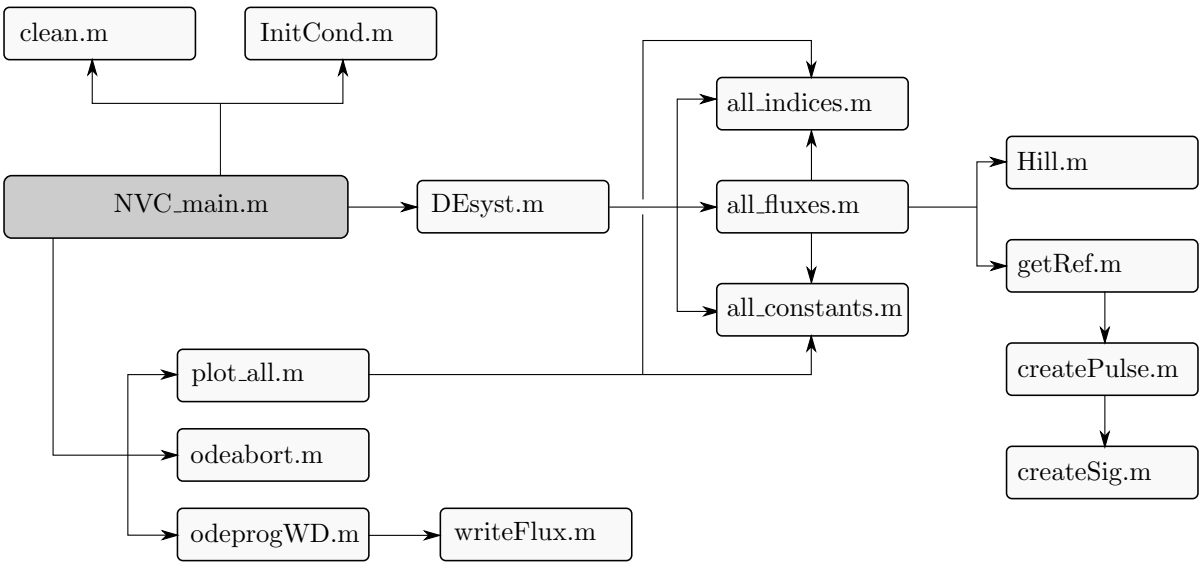

Figure 9: **Diagram to illustrate the code structure.** The main script (*'NVC_main.m'*) calls an ode solver which solves the set of differential equations iteratively and stores the solution of each time step into a data file.

5 Results

5.1 NVU1.1

Potassium input signal (figure 10)

At the top the neuronal K^+ input signal is shown. This input signal is pumped into the SC by the NE. As a result of that, there is more K^+ taken up by the AC in the beginning of the input pulse, and released at the end of the input pulse. In the second graph the membrane potential of the AC is shown over time. When the K^+ concentration in the SC is increased the membrane voltage depolarises and when the K^+ concentration in the SC decreases the membrane potential repolarises again. In the third graph the fluxes into the PVS are shown. In blue the flux by the astrocytic BK channel, and in green the flux by the KIR channel in the SMC is shown. The drop in the middle of the KIR flux is caused because the SMC becomes in a oscillatory state and therefore the efflux by the KIR channel follows the Ca^{2+} waves inside the SMC. The bottom figure shows the K^+ concentration in the PVS.

Solutions of astrocyte and BK-channel equations (figure 11)

The top 4 graphs display the concentrations of K^+, Ca^{2+} IP_3 and EET in the astrocyte. These concentrations, together with the membrane voltage showed in the right bottom graph, all contribute to the opening of the BK-channel in their own way. The open state of the BK channel determines the potassium flux from the astrocyte to the perivascular spcace, where it induces vascular contraction.

SMC and EC fluxes (figure 12 and 13)

In these figures the coupling and the fluxes in the SMC and EC are shown. When one of the fluxes is negative, it means that the direction of the flux is in the opposite than it is defined in the equations. These figures show that when the neuronal signal is given, the VOCC closes and that the SMC goes into an oscillatory state.

Conservation equations (figure 14)

The graphs in this figure shows the solutions of the differential equations of the SMC and EC. The graphs on the left side are the SMC results, and at the right side the EC results. From top to bottom the following parameters are shown over time: the intracellular Ca^{2+} concentration, the IP_3 concentration, the sarcoplasmic (SMC) or endoplasmic (EC) Ca^{2+} concentration, the membrane voltage and at the bottom for the SMC the open probability of the K^+ channels.

Hai and Murphy and radius model (figure 15)

In this figure the fraction of the four states (M, Mp, AMp, AM) of myosin in the SMC are shown at the top. At the bottom left the fraction of attached cross bridged myosin (the sum

of AM and AMp) is shown. And at the bottom right the radius is plotted over time. The increase in vessel diameter is in the expected order of magnitude.

Overview from the synaptic cleft to radius change (figure 16)

This figure descripes the main pathway from the synaptic cleft to the radius change (leaving out the astrocyte equations which can be found in figure 11) It starts with a K^+ concentration in the synaptic cleft, followed by the flux trough the BK-channel determined in the astrocyte, leading to an increased K^+ concentration in the perivascular space. This causes an increased K^+ influx trough the KIR channel, changing the membrane voltage of the SMC. The Ca^{2+} flux through the VOCC increases, decreasing the Ca^{2+} concentration in the SMC and thereby inducing vasodilation.

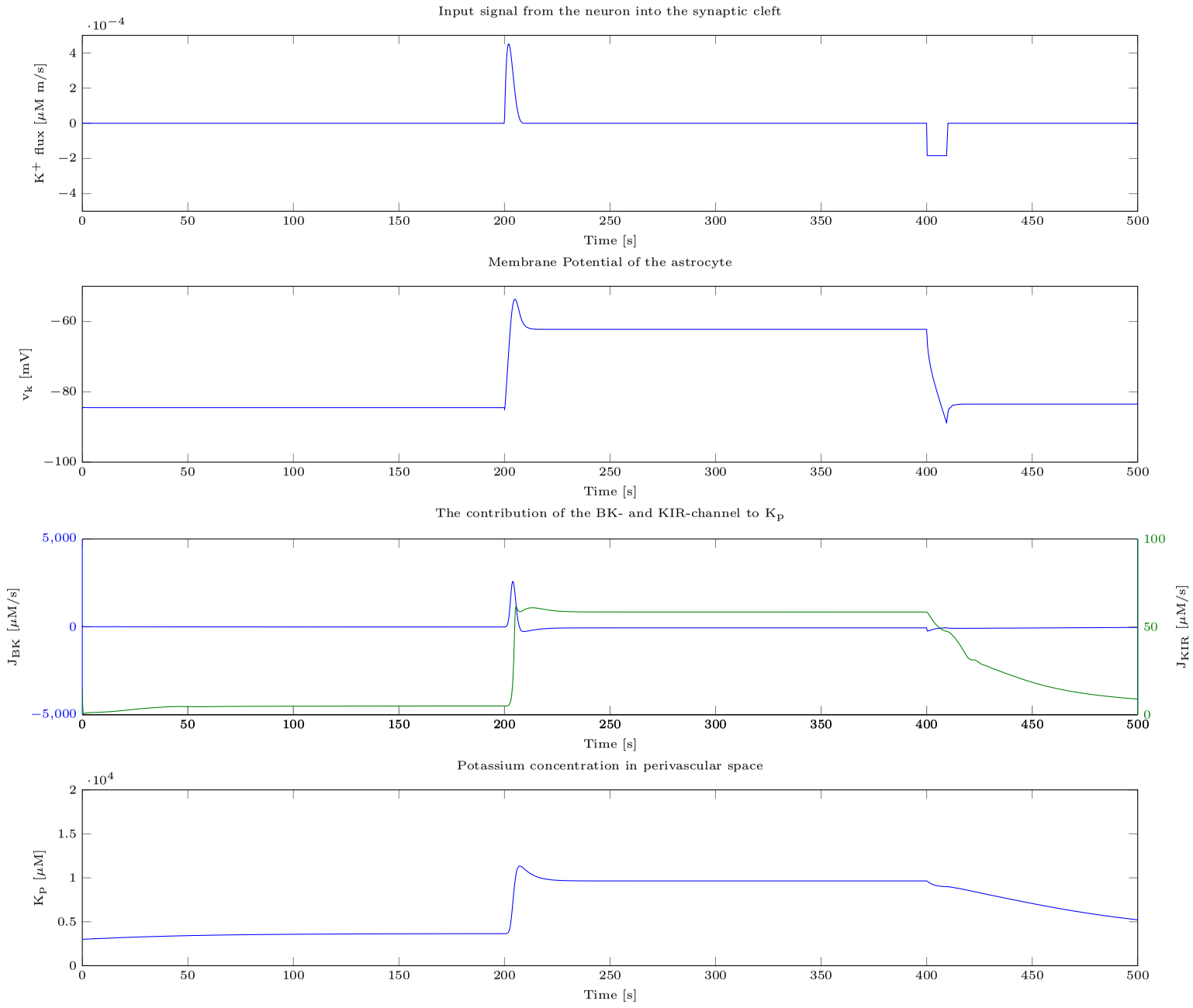

Figure 10: The input signal

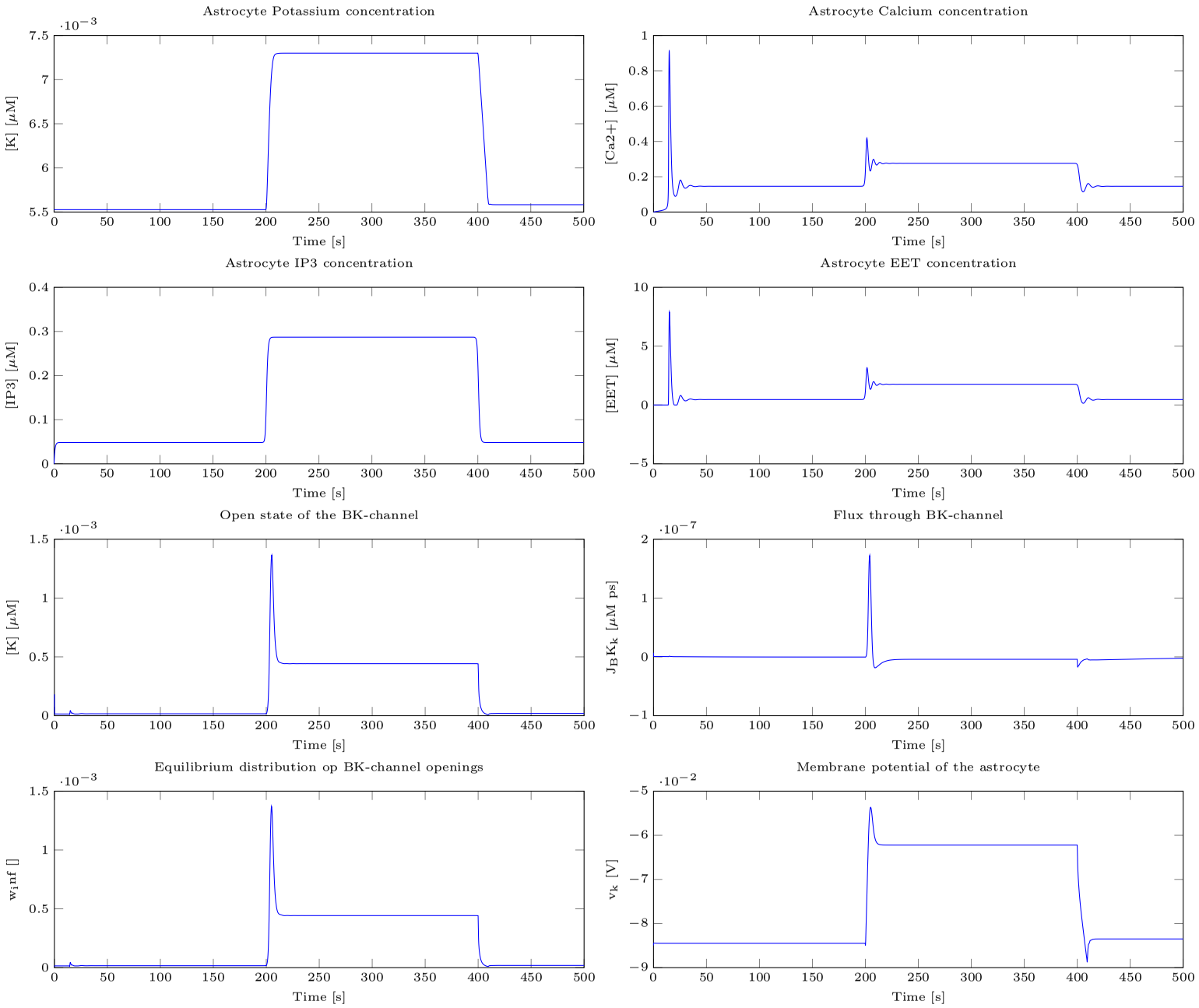

Figure 11: The solutions of astrocytic equations and the BK-channel

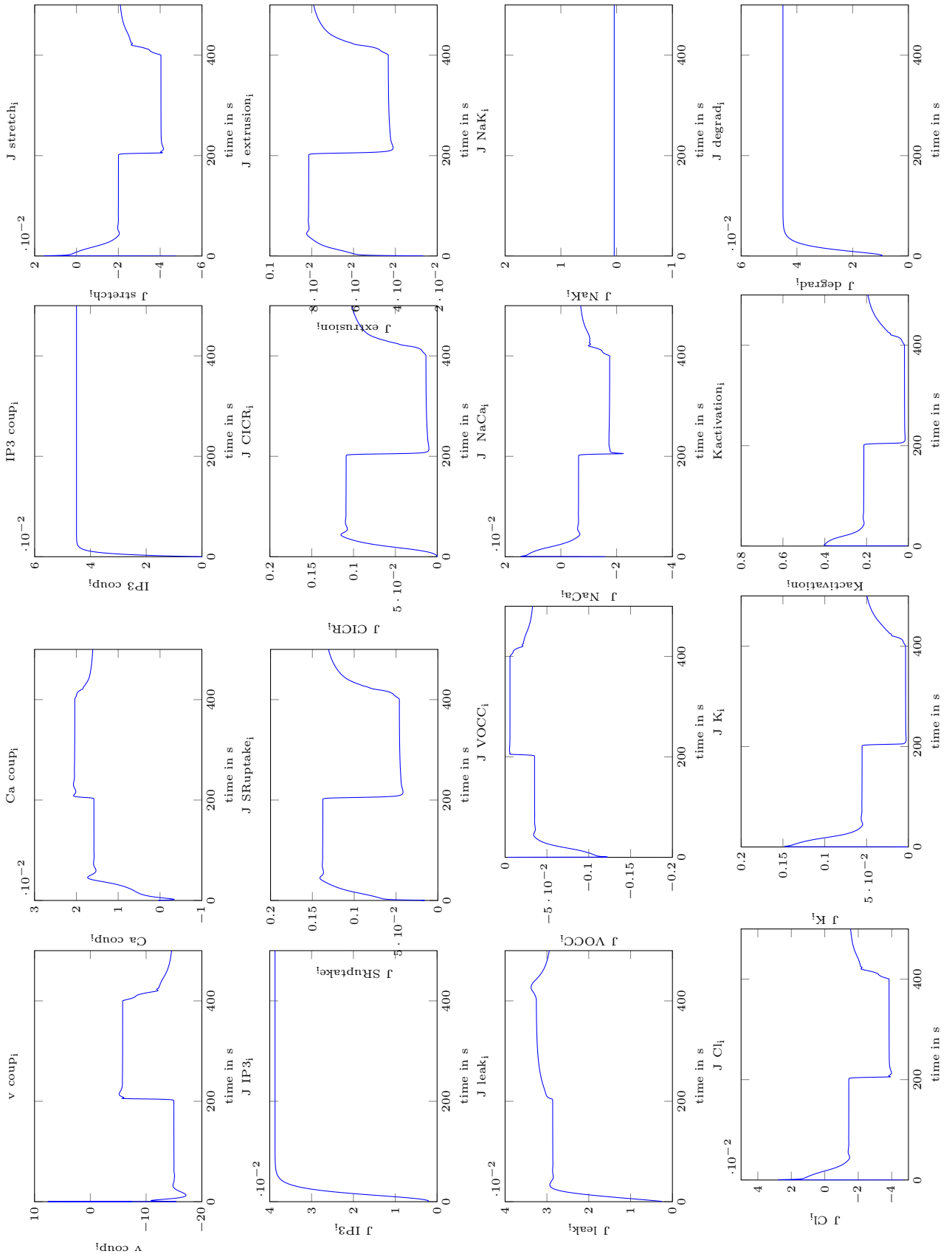

Figure 12: The SMC fluxes

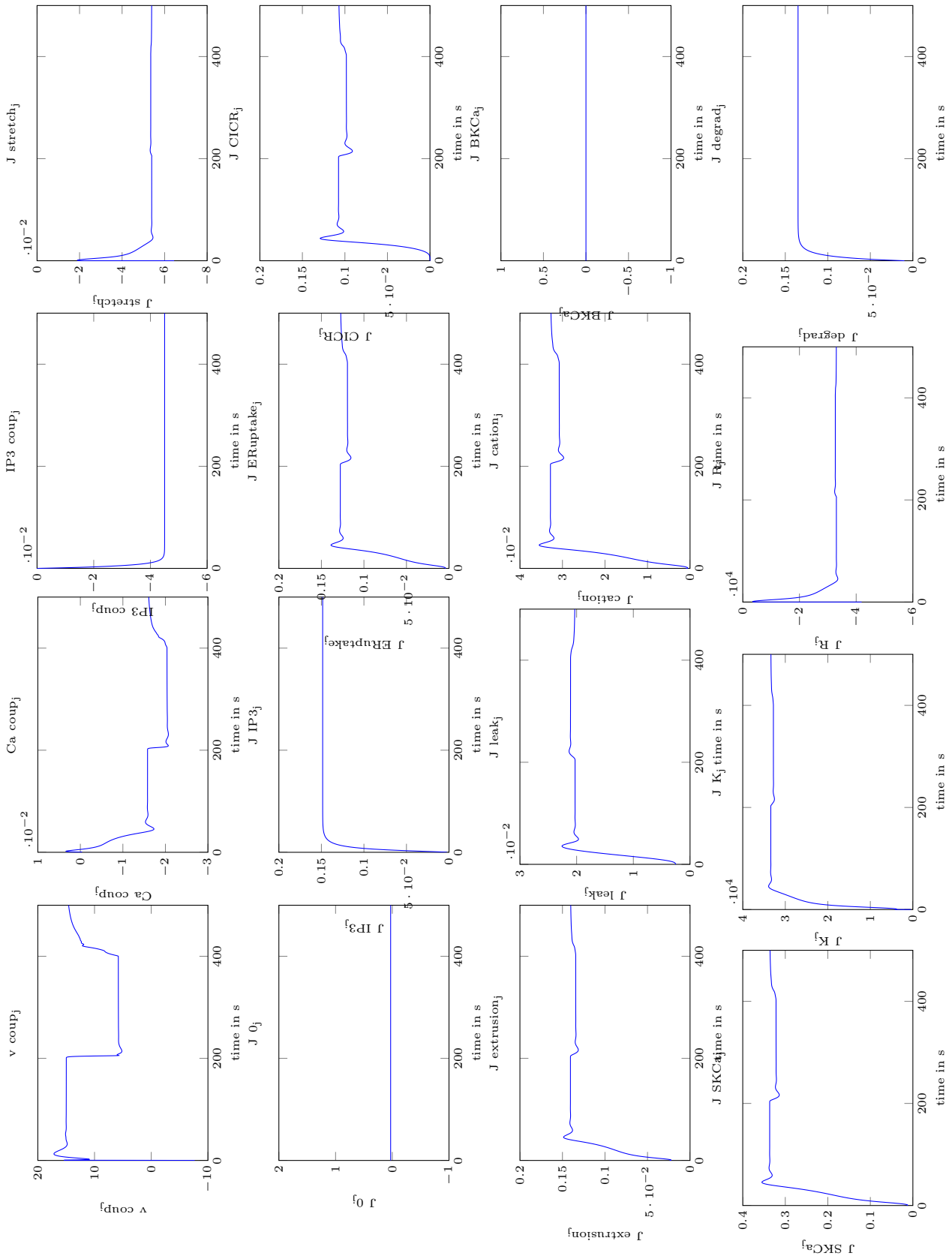

Figure 13: The EC fluxes

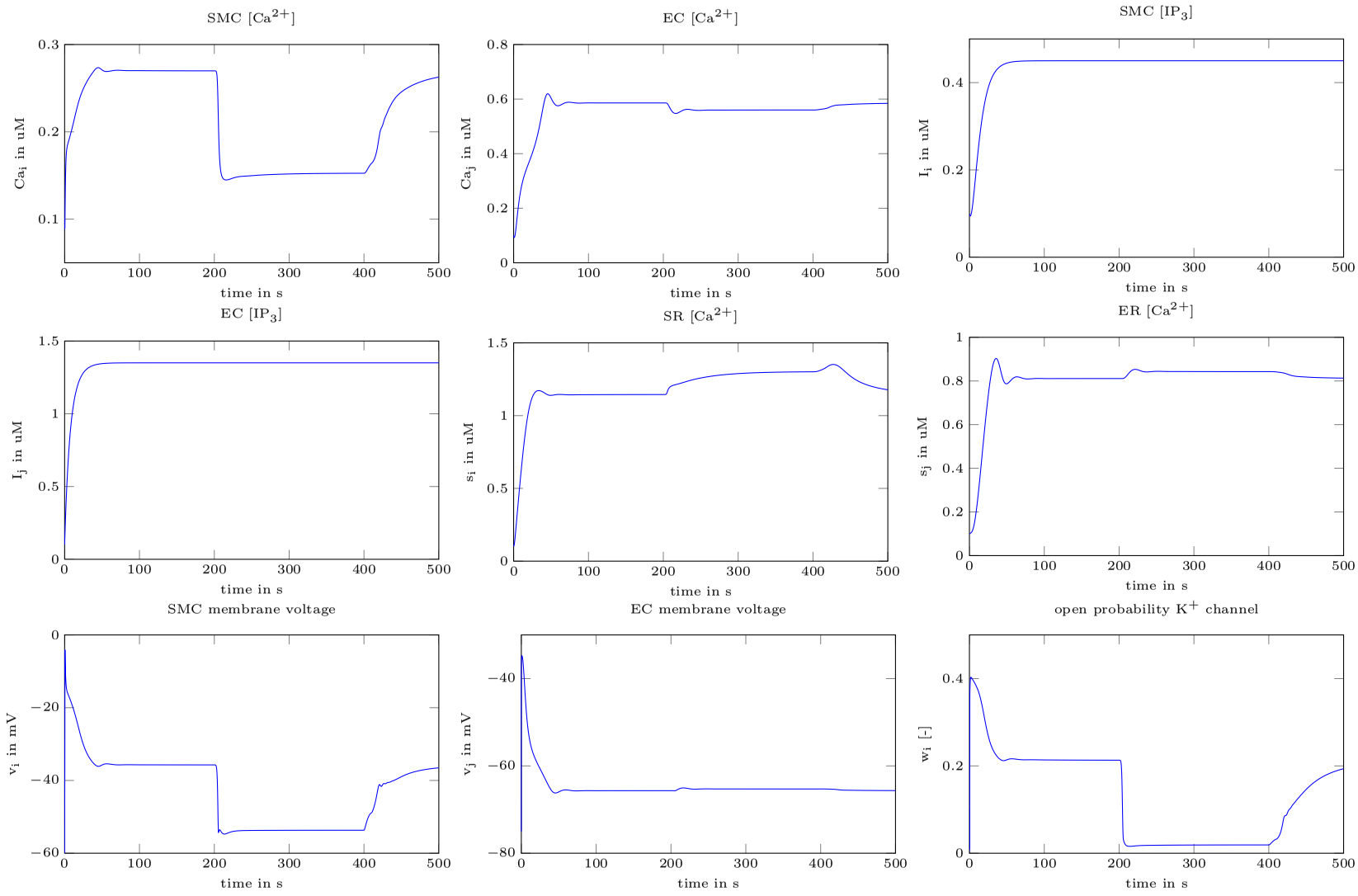

Figure 14: Solutions of the differential equations

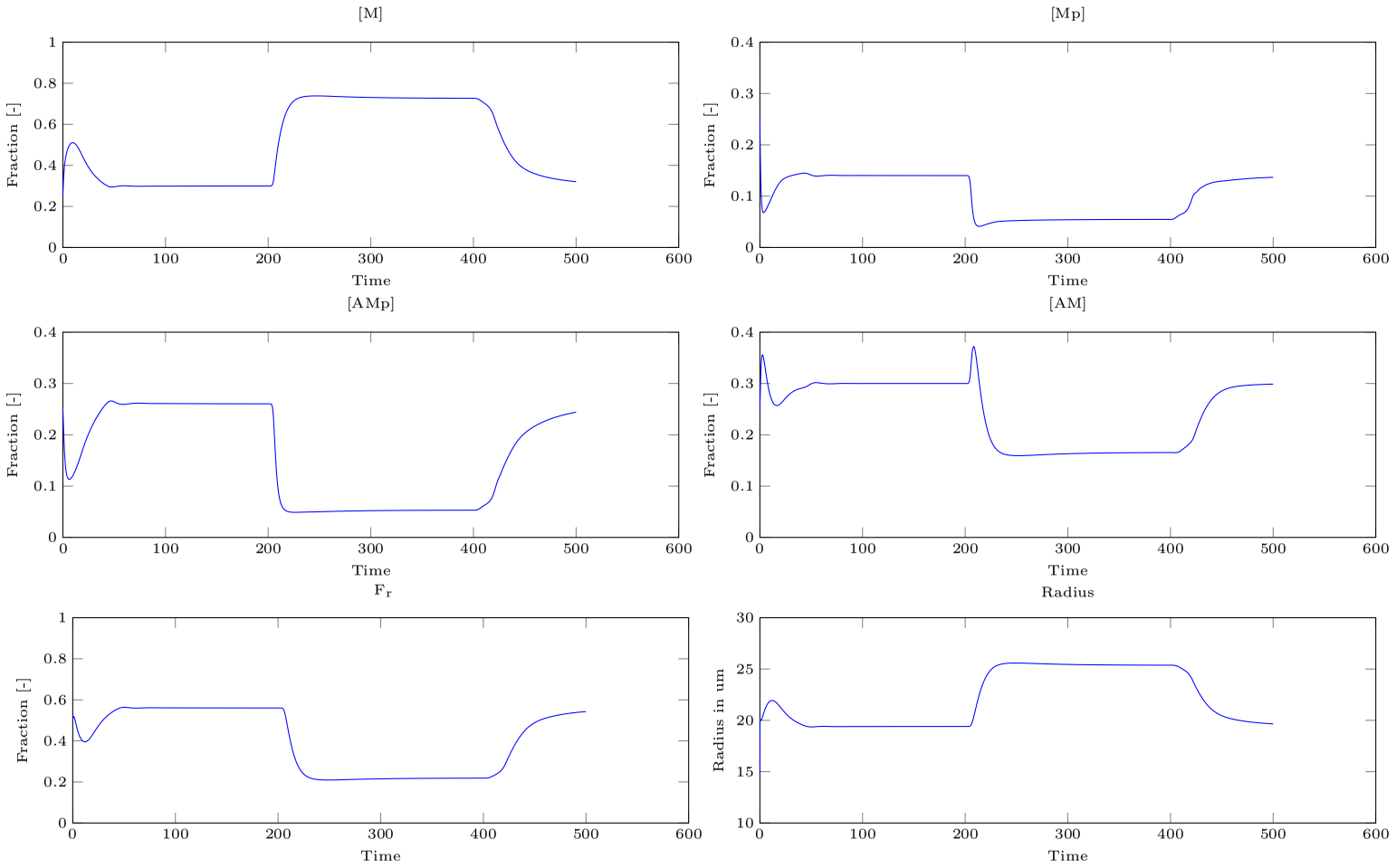

Figure 15: The Myosin Contraction model

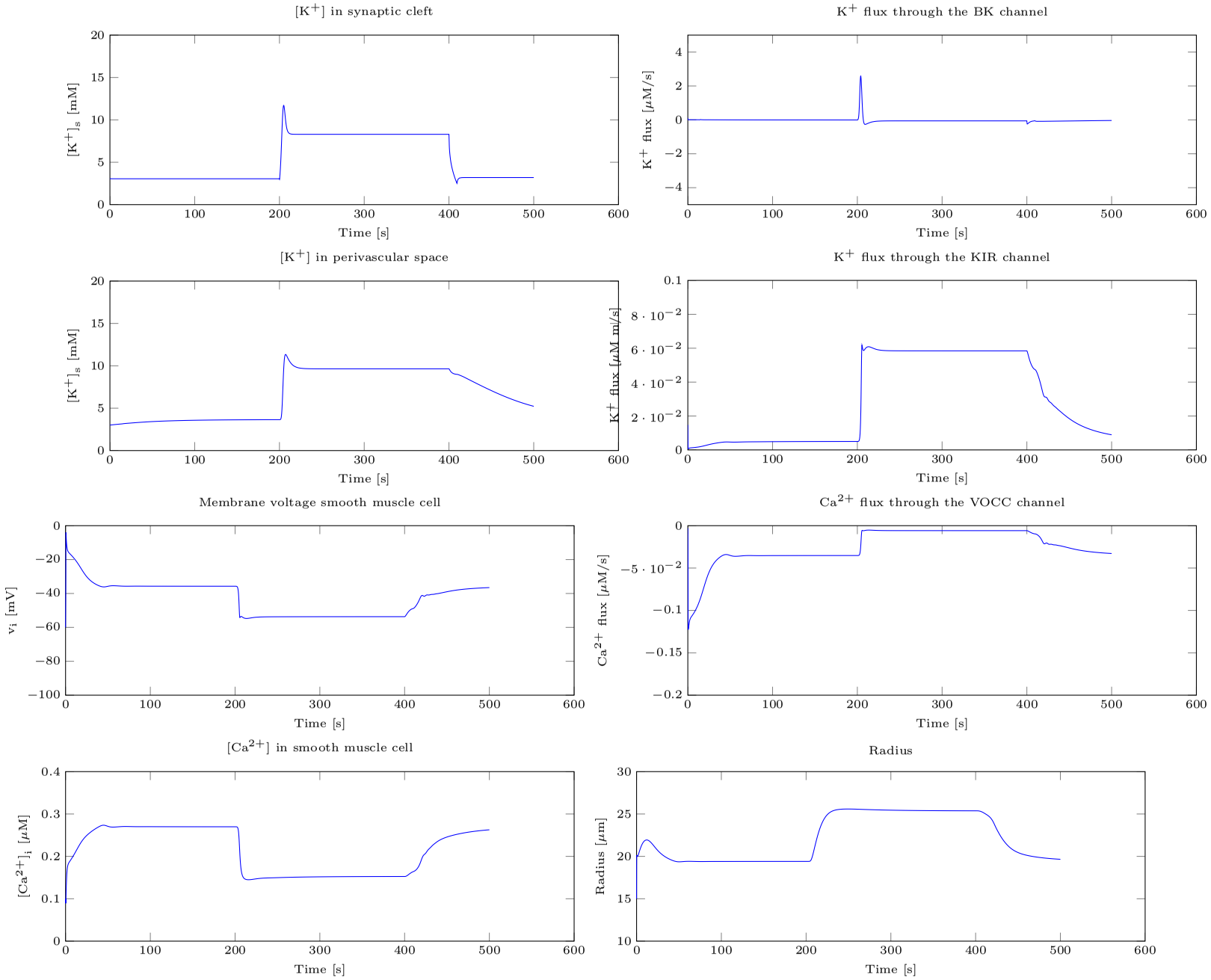

Figure 16: Summary describing effects from the input signal to radius change

5.2 NVU1.1 compared to NVU1.0

The main thing that stands out is the slow outflux of potassium in the perivascular space at the end of the pulse. (figure 17 bottom graph) This change is due to a smaller negative flux in the BK-channel, wich can be seen in figure 18 top right graph. This indicates that with the current calcium and EET concentrations in the astrocyte, there are fewer open BK-channels compared to NVU1.0. Looking at the graphs in figure 18 this means that it takes a longer time to reach the steady state after the end of the pulse, resulting in smoother changes. Furthermore, the slower response has caused the over- and undershoots generated by NVU1.0 to disappear, which makes the results look more physiological. [1]

Figure 19 shows the effects of different regulating mechanisms of the BK-channel. Blue line represents NVU 1.0 (depends only on membrane voltage), red is the result of NVU 1.1 (Depends on membrane voltage, Ca^{2+} concentration and EET concentration), green is NVU 1.1 without the effects of the calcium concentration, and black represents NVU 1.1 without the EET concentration playing a part. The black and green line don't represent physiological situations, but they provide insight in the effects of the separate systems. For the green line the Calcium concentration was simulated (otherwise there would have been no EET), but it was not used in the equations describing the opening of the BK-channel. (v_3 was replaced by the constant used in NVU1.0) The black line does the opposite, the EET voltage shift is ignored (as in NVU 1.0) and v_3 is changed to the Ca^{2+} dependent equation. It can be seen that adding the Ca^{2+} concentration to the equation describing the open state of the BK-channels leads to a decrease in negative flux through the BK-channel, and therefore leads to a slow restoration process. The EET concentration dependent voltage shift, contributing to the open state of the BK-channel has the opposite effect. It increases the negative K^+ flux torugh the BK-channel, creating similar results as NVU 1.0. The combination of these two effects (NVU 1.1) shows results that lay somewhere in between the previous results, generating a stable return to the steady state at a more realistic speed.

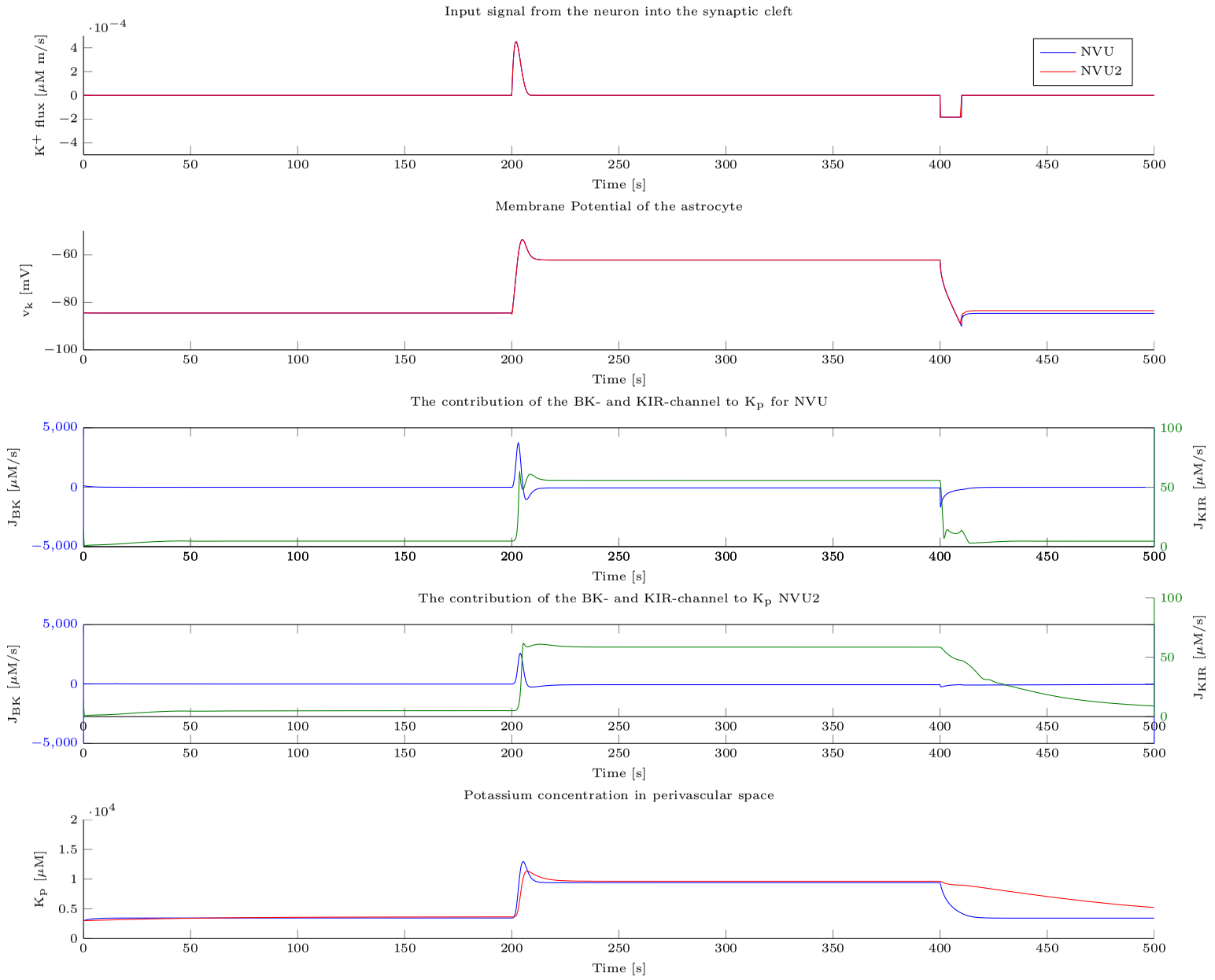

Figure 17: Overview 1, differences between NVU 1.1 & 1.0

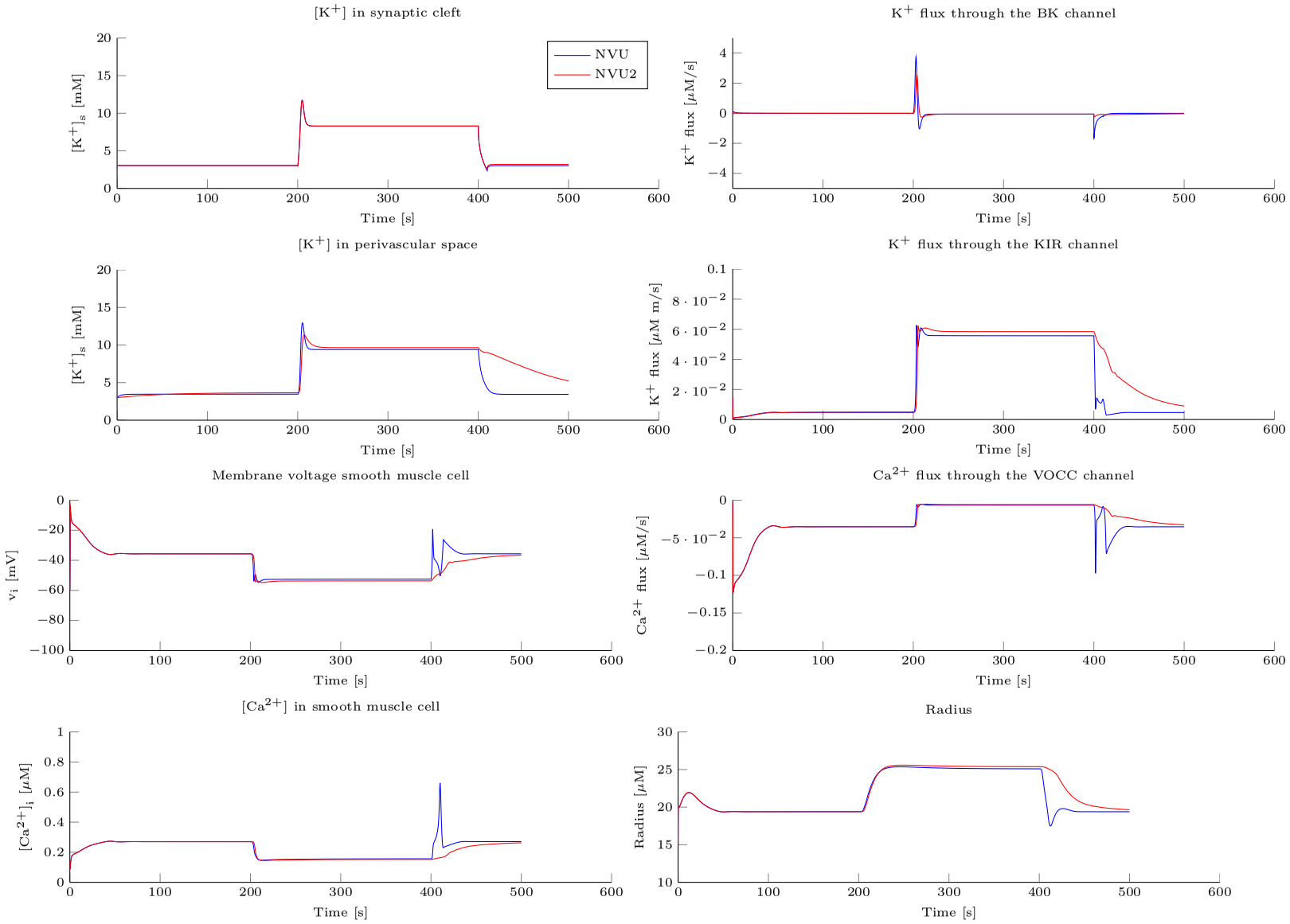

Figure 18: Overview 2, differences between NVU 1.1 & 1.0

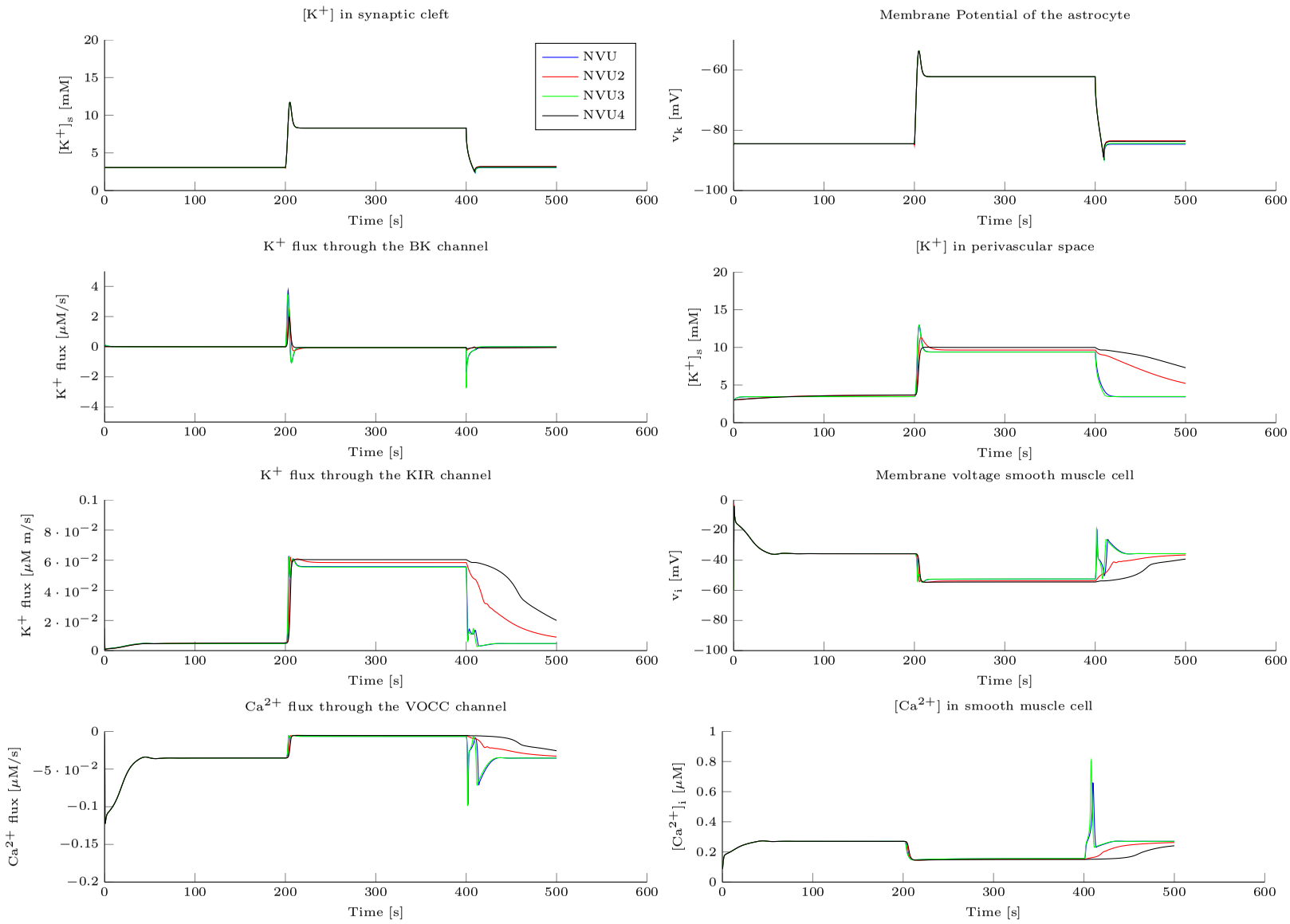

Figure 19: The effects of different regulation of the BK-channel

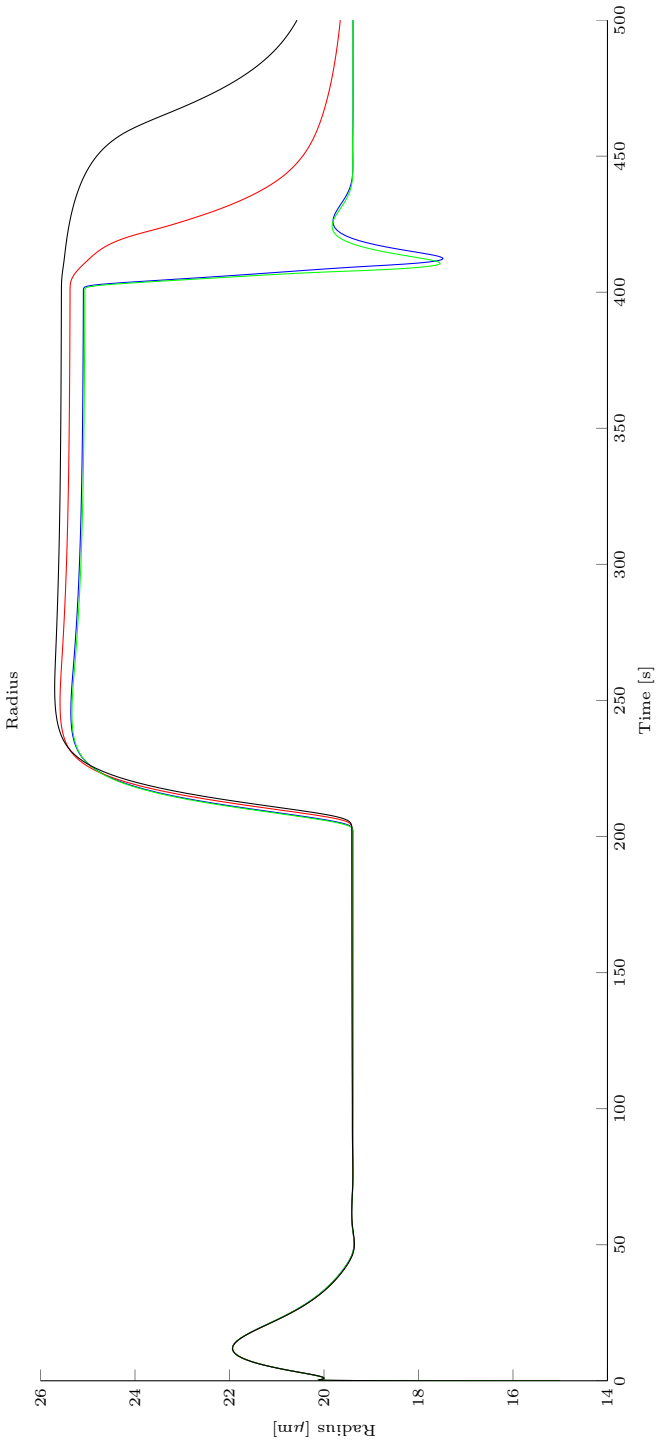

Figure 20: Radius change for different BK-channel regulations

6 Release notes

6.1 Adaptations to the astrocyte model

In the creation of NVU 1.1 the work of Farr& David(2011) [3] was implemented in NVU 1.0. This means that several pathways were added and equations were combined. First a glutamate release in the synaptic cleft was simulated by creating a smooth pulse function, ρ, describing the ratio of bound to total glutamate receptors on the synapse end of the astrocyte. This induces an IP_3 release into the cell, causing the release of Calcium from the ER into the cytosol, which on his turn leads to the production of EET. The open state of the BK-channels in NVU 1.0 depends only on the membrane voltage, in NVU 1.1 the opening of BK-channels is regulated by the membrane voltage as well as the EET and Ca^{2+} concentration. Furthermore, several corrections, proposed by de Kock & van der Donck (2013) [2], on the model by Farr were included. These corrections include an equation to describe the buffering parameter in the Ca^{2+} conservation equation (Farr [3] used a constant to describe this parameter) and some changes in parameter values.

6.2 New/changed equations & parameters for the astrocyte model

ρ input signal The smooth pulse function ρ

$$\rho(t) = \frac{Amp - base}{2} \times \left(1 + \tanh\left(\frac{t - t_0}{\theta_L}\right)\right) + base + \frac{Amp - base}{2} \times \left(1 + \tanh\left(\frac{t - t_2}{\theta_R}\right)\right) + base - Amp \tag{96}$$

Amp	Amplitude of smooth pulse function	0.7	ME
$base$	Baseline of smooth pulse function	0.1	ME
θ_L	Left ramp of smooth pulse function	1	ME
θ_R	Left ramp of smooth pulse function	1	ME

6.2.1 Conservation Equations

Ca^{2+} concentration in the astrocytic cytosol:

$$\frac{\mathrm{d}c_k}{\mathrm{d}t} = B_{\mathrm{cyt}}(J_{\mathrm{IP_3}} - J_{\mathrm{pump}} + J_{\mathrm{ER_leak}}) \tag{97}$$

Ca^{2+} concentration in the astrocytic ER:

$$\frac{\mathrm{d}s_k}{\mathrm{d}t} = \frac{1}{VR_{\mathrm{ER_{cyt}}}}(\frac{dc_k}{dt}) \tag{98}$$

The inactivation variable for IP_3:

$$\frac{\mathrm{d}h_k}{\mathrm{d}t} = k_{\mathrm{on}}[K_{\mathrm{inh}} - (c_k + K_{\mathrm{inh}})h_k] \tag{99}$$

The IP_3 concentration:

$$\frac{\mathrm{d}i_k}{\mathrm{d}t} = r_h G - k_{\mathrm{deg}} i_k \tag{100}$$

The EET concentration:

$$\frac{\mathrm{d}eetk_k}{\mathrm{d}t} = V_{\mathrm{eet}}(c_k - c_{\mathrm{k,min}}) - k_{\mathrm{eet}} eet_k \tag{101}$$

Open probability of the BK channel (s^{-1}):

$$\frac{\mathrm{d}w_k}{\mathrm{d}t} = \phi_w \left(w_\infty - w_k\right) \tag{102}$$

$VR_{\mathrm{ER_{cyt}}}$	Volume ratio of the ER to the cytosol in the astrocyte	0.185 [-]	[3]
k_{on}	Rate of Ca^{2+} binding to the IP_3R	2 [µM s^{-1}]	[3]
K_{inh}	Dissociation rate of k_{on}	[0.1µM]	[3]
r_h	Maximum rate of IP_3 production in the astrocyte	4.8 [µM]	[3]
k_{deg}	Rate constant for IP_3 degradation	1.25 [s^{-1}]	[3]
V_{eet}	Rate constant for EET production	72[µM]	[3]
k_{eet}	Rate constant for EET degradation	7.2[µM]	[3]
$c_{\mathrm{k,min}}$	Minimum Ca^{2+} concentration required for EET production	0.1 [uM]	[3]

6.2.2 Fluxes

Ca^{2+} flux from the ER to the cytosol in the astrocyte through IP_3 Receptors (IP_3R) by IP_3:

$$J_{\mathrm{IP3}} = J_{\mathrm{max}}[(\frac{i_k}{i_k + K_i})(\frac{c_k}{c_k + K_{\mathrm{act}}})h_k]^3 \times [1 - \frac{c_k}{s_k}] \tag{103}$$

The leakage Ca^{2+} flux from the ER to the cytosol in the astrocyte:

$$J_{\mathrm{ER_leak}} = P_L(1 - \frac{c_k}{s_k}) \tag{104}$$

The ATP dependent Ca^{2+} pump flux from the cytoplasm to the ER in the astrocyte:

$$J_{\mathrm{pump}} = V_{\mathrm{max}} \frac{c_k^2}{c_k^2 + k_p ump^2} \tag{105}$$

J_{max}	Maximum IP_3 rate	2880 µM s^{-1}	[3]
K_I	Dissociation constant for IP_3 binding to IP_3R	0.03 µM	[3]
K_{act}	Dissociation constant for Ca^{2+} binding to IP_3R	0.17 µM	[3]
P_L	Associated with the steady state Ca^{2+} balance	0.0842 µM	[2]
V_{max}	Maximal pumping rate of the Ca^{2+} pump	20 µM s^{-1}	[3]
k_{pump}	Dissociation constant of the Ca^{2+} pump	0.24 µM	[3]

6.2.3 Additional equations

The Calcium buffering parameter in the astrocytic cytosol (-)

$$B_{cyt} = \left(1 + BK_{end} + \frac{K_{ex}B_{ex}}{(K_{ex} + c_k)^2}\right)^{-1} \tag{106}$$

The ratio of active to total G-protein (-)

$$G = \frac{\rho + \delta}{K_g + \rho + \delta} \tag{107}$$

Equilibrium state BK-channel (-):

$$w_\infty = 0.5\left(1 + \tanh\left(\frac{v_k + (eet_{\text{shift}}eet_k) - v_3}{v_4}\right)\right) \tag{108}$$

The time constant associated with the opening of BK channels (in s^{-1}):

$$\phi_w = \psi_w \cosh\left(\frac{v_k - v_3}{2v_4}\right) \tag{109}$$

Ca^{2+} dependent shift of the opening of the BK-channels

$$v_3 = \frac{v_5}{2}\tanh\left(\frac{c_k - Ca_3}{Ca_4}\right) + v_6 \tag{110}$$

BK_{end}	Cytosolic endogenous buffer constant	40 [-]	[2]
K_{ex}	Cytosolic exogenous buffer dissociation constant	0.26 [µM]	[2]
B_{ex}	Concentration of cytosolic exogenous buffer	11.35 [µM]	[2]
δ	Ratio of the activities of the bound and unbound receptors	1.235e-3 [-]	[3]
K_G	The G-protein dissociation constant	8.82 [-]	[3]
v_4	A measure of the spread of the distribution of the open probability of the BK channel	14.5e-3 [V]	[6]
v_5	Determines the range of the shift of n_{inf} as calcium varies	8e-3 [V]	[3]
v_6	The voltage associated with the opening of half the population	-15e-3 [V]	[3]
ψ_w	A characteristic time for the open probability of the BK channel	2.664 [s^{-1}]	[6]

References

[1] Brenda R Chen, Matthew B Bouchard, Addason FH McCaslin, Sean A Burgess, and Elizabeth Hillman. High-speed vascular dynamics of the hemodynamic response. *Neuroimage*, 54(2):1021–1030, 2011.

[2] L Van Der Donk and E. G. J. DE Kock. Bluefern Supercomputing Unit University of Canterbury Eindhoven University of Technology. 2013.

[3] Hannah Farr and Tim David. Models of neurovascular coupling via potassium and EET signalling. *Journal of theoretical biology*, 286(1):13–23, October 2011. ISSN 1095-8541. doi: 10.1016/j.jtbi.2011.07.006. URL `http://www.ncbi.nlm.nih.gov/pubmed/21781976`.

[4] Jessica a Filosa, Adrian D Bonev, and Mark T Nelson. Calcium dynamics in cortical astrocytes and arterioles during neurovascular coupling. *Circulation research*, 95(10): e73–81, November 2004. ISSN 1524-4571. doi: 10.1161/01.RES.0000148636.60732.2e. URL `http://www.ncbi.nlm.nih.gov/pubmed/15499024`.

[5] T Franklin, V Tech, J Norris, and W Forrest. A MATLAB ODE progress display function with interrupt control. 2006.

[6] J M Gonzalez-Fernandez and B Ermentrout. On the origin and dynamics of the vasomotion of small arteries. *Mathematical biosciences*, 119(2):127–167, 1994.

[7] R Gore and M Davis. Mechanics of Smooth Muscle in isolated single Microvessels. *Annals of Biomedical Engineering*, 12:511–520, 1984.

[8] C Hai and R A Murphy. Ca2+ Crossbridge Phosphorylation, and Contraction. *Annual review of physiology*, 51(1):285–298, 1989.

[9] Michèle Koenigsberger, Roger Sauser, Jean-Louis Bény, and Jean-Jacques Meister. Role of the Endothelium on Arterial Vasomotion. *Biophysical Journal*, 88(6):3845–3854, June 2005. ISSN 0006-3495. doi: 10.1529/biophysj.104.054965. URL `http://www.pubmedcentral.nih.gov/articlerender.fcgi?artid=1305618&tool=pmcentrez&rendertype=abstract`.

[10] Michèle Koenigsberger, Roger Sauser, Jean-Louis Bény, and Jean-Jacques Meister. Role of the Endothelium on Arterial Vasomotion. *Biophysical Journal*, 88(6):3845–3854, June 2006. ISSN 0006-3495. doi: 10.1529/biophysj.104.054965. URL `http://www.pubmedcentral.nih.gov/articlerender.fcgi?artid=1305618&tool=pmcentrez&rendertype=abstract`.

[11] Ivar Østby, Leiv Øyehaug, Gaute T Einevoll, Erlend a Nagelhus, Erik Plahte, Thomas Zeuthen, Catherine M Lloyd, Ole P Ottersen, and Stig W Omholt. Astrocytic mechanisms explaining neural-activity-induced shrinkage of extraneuronal space. *PLoS com-*

putational biology, 5(1):e1000272, January 2009. ISSN 1553-7358. doi: 10.1371/journal.pcbi.1000272.

[12] Stewart Shipp. Structure and function of the cerebral cortex. *Current biology : CB*, 17(12):R443–9, June 2007. ISSN 0960-9822. doi: 10.1016/j.cub.2007.03.044. URL `http://www.ncbi.nlm.nih.gov/pubmed/17580069`.